





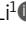






ARTICLE

Hepatic Gadd45 β promotes hyperglycemia and glucose intolerance through DNA demethylation of PGC-1 α

Ling Wu^{1,2*} , Yang Jiao^{3*} , Yao Li^{2*} , Jingjing Jiang³ , Lin Zhao³ , Menghui Li¹ , Bin Li¹ , Zheng Yan¹ , Xuejin Chen² , Xiaoying Li³ , and Yan Lu³ 

Although widely used for their potent anti-inflammatory and immunosuppressive properties, the prescription of glucocorticoid analogues (e.g., dexamethasone) has been associated with deleterious glucose metabolism, compromising their long-term therapeutic use. However, the molecular mechanism remains poorly understood. In the present study, through transcriptomic and epigenomic analysis of two mouse models, we identified a growth arrest and DNA damage-inducible β (Gadd45 β)-dependent pathway that stimulates hepatic glucose production (HGP). Functional studies showed that overexpression of Gadd45 β in vivo or in cultured hepatocytes activates gluconeogenesis and increases HGP. In contrast, liver-specific Gadd45 β -knockout mice were resistant to high-fat diet- or steroid-induced hyperglycemia. Of pathophysiological significance, hepatic Gadd45 β expression is up-regulated in several mouse models of obesity and diabetic patients. Mechanistically, Gadd45 β promotes DNA demethylation of PGC-1 α promoter in conjunction with TET1, thereby stimulating PGC-1 α expression to promote gluconeogenesis and hyperglycemia. Collectively, these findings unveil an epigenomic signature involving Gadd45 β /TET1/DNA demethylation in hepatic glucose metabolism, enabling the identification of pathogenic factors in diabetes.

Introduction

The liver is a dynamic organ that plays a key role in the regulation of systemic glucose metabolism. During periods of nutrient deprivation, the liver is the main source responsible for maintaining euglycemia through hepatic glucose production (HGP). HGP consists of glycogenolysis and gluconeogenesis, which breaks down glycogen and de novo synthesizes glucose from noncarbohydrate precursors, respectively (Petersen et al., 2017). In the fasted state, hepatic gluconeogenesis is activated to maintain blood glucose levels within a normal range, ensuring enough energy supply for glucose-dependent tissues like the brain. However, uncontrolled gluconeogenesis is believed to be one of the major factors that contribute to hyperglycemia and glucose intolerance in obesity and type 2 diabetes mellitus (T2DM). Therefore, inhibiting HGP, especially by decreasing gluconeogenesis, is a potentially appealing avenue for the treatment of diabetes (Rines et al., 2016).

The rate of hepatic gluconeogenesis is mainly controlled by the pancreatic hormone glucagon and adrenal hormone glucocorticoids (GCs). Glucagon activates the cAMP/protein kinase

A/cAMP-responsive element binding protein (CREB) signaling pathway, while GCs activate the nuclear receptor glucocorticoid receptor (GR; Goldstein and Hager, 2015). These two signals act either independently or synergistically to activate many transcription factors (e.g., hepatocyte nuclear factor 4 α [HNF4 α], FoxO1, KLF15, and CREB protein H) that stimulate the expression of two key gluconeogenic enzymes: phosphoenolpyruvate carboxykinase (PEPCK) and glucose-6-phosphatase (G6Pase; Goldstein and Hager, 2015). Of interest, proper metabolic gene regulation and the transactivation of transcription factors require the recruitment of coregulatory proteins (Mouchiroud et al., 2014), such as peroxisome proliferator-activated receptor γ coactivator-1 α (PGC-1 α). The gluconeogenic effect of PGC-1 α is achieved by directly coactivating HNF4 α and FoxO1, leading to an increase in the transcription of gluconeogenic genes and HGP (Lin et al., 2005; Piccinin et al., 2019). In contrast, both PGC-1 α -KO mice and acute liver-specific PGC-1 α -knockdown mice displayed hypoglycemia under a fasted state (Lin et al., 2004; Koo et al., 2004). Moreover, hepatic PGC-1 α is markedly

¹Department of Assisted Reproduction, Shanghai Ninth People's Hospital, Shanghai Jiao Tong University School of Medicine, Shanghai, China; ²Department of Laboratory Animal Science, Shanghai Jiao Tong University School of Medicine, Shanghai, China; ³Key Laboratory of Metabolism and Molecular Medicine, Ministry of Education, Department of Endocrinology and Metabolism, Zhongshan Hospital, Fudan University, Shanghai, China.

*L. Wu, Y. Jiao, and Y. Li contributed equally to this work; Correspondence to Yan Lu: lu.yan2@zs-hospital.sh.cn.

© 2021 Wu et al. This article is distributed under the terms of an Attribution-Noncommercial-Share Alike-No Mirror Sites license for the first six months after the publication date (see <http://www.rupress.org/terms/>). After six months it is available under a Creative Commons License (Attribution-Noncommercial-Share Alike 4.0 International license, as described at <https://creativecommons.org/licenses/by-nc-sa/4.0/>).

up-regulated in multiple models of diabetes (Yoon et al., 2001), and selective chemical inhibition of PGC-1 α suppressed hepatic gluconeogenesis and alleviated hyperglycemia in diabetic mice (Sharabi et al., 2017), highlighting its importance in systemic glucose homeostasis. In addition to the transcriptional regulation, epigenetic changes, including DNA methylation and histone modifications, emerge as an important signature involved in reprogramming of metabolic pathways (Ling and Rönn, 2019). For instance, alterations in DNA methylation of multiple gene loci have been linked to the development of obesity and T2DM by epigenome-wide association studies (Wahl et al., 2017). Besides, specific expression and methylation differences were observed for several genes coding metabolic enzymes between distinct liver phenotypes (Ahrens et al., 2013). Nevertheless, our understanding of the importance of epigenetic function in the hepatic gluconeogenesis and HGP is relatively limited.

In the present study, we sought to explore the role of the epigenome in HGP using two mouse models of HGP: dexamethasone (Dex)-treated mice and fasted mice. Dex and other synthetic GC analogues have been used clinically for decades to treat many types of autoimmune diseases as anti-inflammatory drugs and also employed to prevent organ transplant rejection as immunosuppressants. Unfortunately, elevated GC levels are associated with hyperglycemia and glucose intolerance, which becomes one of the key limitations of the long-term use of GC drugs (Rose and Herzig, 2013). As a result, we found that both Dex treatment and fasting induce the expression of growth arrest and DNA damage-inducible β (Gadd45 β), which has been implicated in the active DNA demethylation of specific loci in vertebrates (Ma et al., 2009; Schüle et al., 2019). Using liver-specific Gadd45 β overexpression and deficient mice, we further demonstrate the physiological and pathological significance of Gadd45 β -mediated gluconeogenesis. Our results illustrate an example of how hepatic epigenetic changes coordinate HGP and systemic glucose homeostasis, which may have important implications for the treatment of diabetes, including steroid-associated diabetes.

Results

Identification of Gadd45 β as a regulator of hepatic gluconeogenesis

To identify potential genes that may contribute to the development of GC-associated hyperglycemia, we performed RNA sequencing (RNA-seq) analysis of the livers collected from two mouse models (Fig. S1, A and B). In the first model, C57BL/6 mice were treated with Dex (1.0 mg/kg) daily for 14 d (Fig. S1 A). This dose of Dex has been shown to cause hyperglycemia in mice by our previous work (Lu et al., 2012). In the second model, C57BL/6 mice were fed ad libitum or were fasted for 16 h (Fig. S1 B). Differentially expressed genes were identified using a q value <0.05 and fold change >1.5. The q value is an adjusted P value, taking into account the false discovery rate. In the livers of Dex-treated mice, 1,107 genes were significantly differentially expressed compared with control mice. Of these genes, 129 showed increased expression, and 978 showed decreased expression. As expected, Dex treatment induced the expression of gluconeogenic

genes, such as Pparg1a (coding PGC-1 α) and Pck1 (coding PEPCK; Table S1). Besides, the most highly up-regulated genes included a range of novel genes but also those known to be regulated by GCs, such as Cyp2b10 (Jarukamjorn et al., 2001), Mt2 (Wray et al., 2019), and Lcn2 (Owen et al., 2008; Table S1). In fasted livers, 612 genes were significantly differentially regulated compared with the livers of ad libitum-fed mice. Of these genes, 207 were up-regulated, and 405 were down-regulated. When comparing both mouse models, we identified 21 genes that were commonly up-regulated and 56 genes that were commonly down-regulated (Fig. S1, C and D; and Table S2 and Table S3).

Of note, our screen revealed a pronounced up-regulation of Gadd45 β in the livers of Dex-treated and fasted mice compared with the corresponding controls (Table S2). Increased Gadd45 β expression in both mouse models was further confirmed by quantitative real-time PCR (qRT-PCR), which showed a 21.76-fold up-regulation of Gadd45 β expression in the livers of Dex-treated mice and an 8.98-fold up-regulation of Gadd45 β expression in the livers of fasted mice (Fig. 1 A and Fig. S1 E). Western blotting analysis confirmed that hepatic Gadd45 β protein was up-regulated in both models (Fig. 1 B and Fig. S1 F). In contrast, expression levels of Gadd45 α and Gadd45 γ , two other members of the Gadd45 family, were not affected by Dex or fasting (Fig. S1, G and H). Moreover, qRT-PCR and Western blotting analysis showed that the mRNA and protein levels of Gadd45 β were increased in mouse primary hepatocytes (MPHs) following exposure to Dex (Fig. 1, C and D). Furthermore, we observed a dose-dependent induction in Gadd45 β mRNA expression following Dex treatment (Fig. S1 I). Time-course experiments revealed that Gadd45 β mRNA expression was rapidly induced in MPHs: in as little as 30 min, expression was significantly increased over baseline levels (Fig. S1 J).

Gluconeogenesis can also be induced by glucagon, chronic inflammation, and persistent ER stress. Thus, we examined the ability of forskolin (which mimics glucagon), TNF α (which mimics chronic inflammation), and tunicamycin (which mimics ER stress) to activate Gadd45 β expression. As a result, these factors failed to up-regulate Gadd45 β expression in MPHs (Fig. S1, K–M). Therefore, Gadd45 β may specifically respond to steroid hormone signaling in the process of hepatic gluconeogenesis.

Activation of the GC–GR signaling pathway up-regulates Gadd45 β expression

The effects of GCs are mediated through activation of the GR, a member of the nuclear hormone receptor superfamily. Treatment with low-dose RU486, a dual antagonist of GRs and progesterone receptors (PRs), decreased Dex-induced Gadd45 β expression in MPHs, and high-dose RU486 almost completely blocked it (Fig. 1 E). Given that PR expression is absent in hepatocytes (Lu et al., 2020; Yang et al., 2006), the effects of RU486 suggest that the transactivation of Gadd45 β by Dex is mediated by the GR. These results were confirmed by adenoviral shRNA targeting of the GR. Knockdown of endogenous GR reduced basal Gadd45 β expression and attenuated Dex-mediated induction of Gadd45 β in MPHs (Fig. 1 F).

To further demonstrate the role of the GC–GR axis in the regulation of Gadd45 β , C57BL/6 mice were administered GR

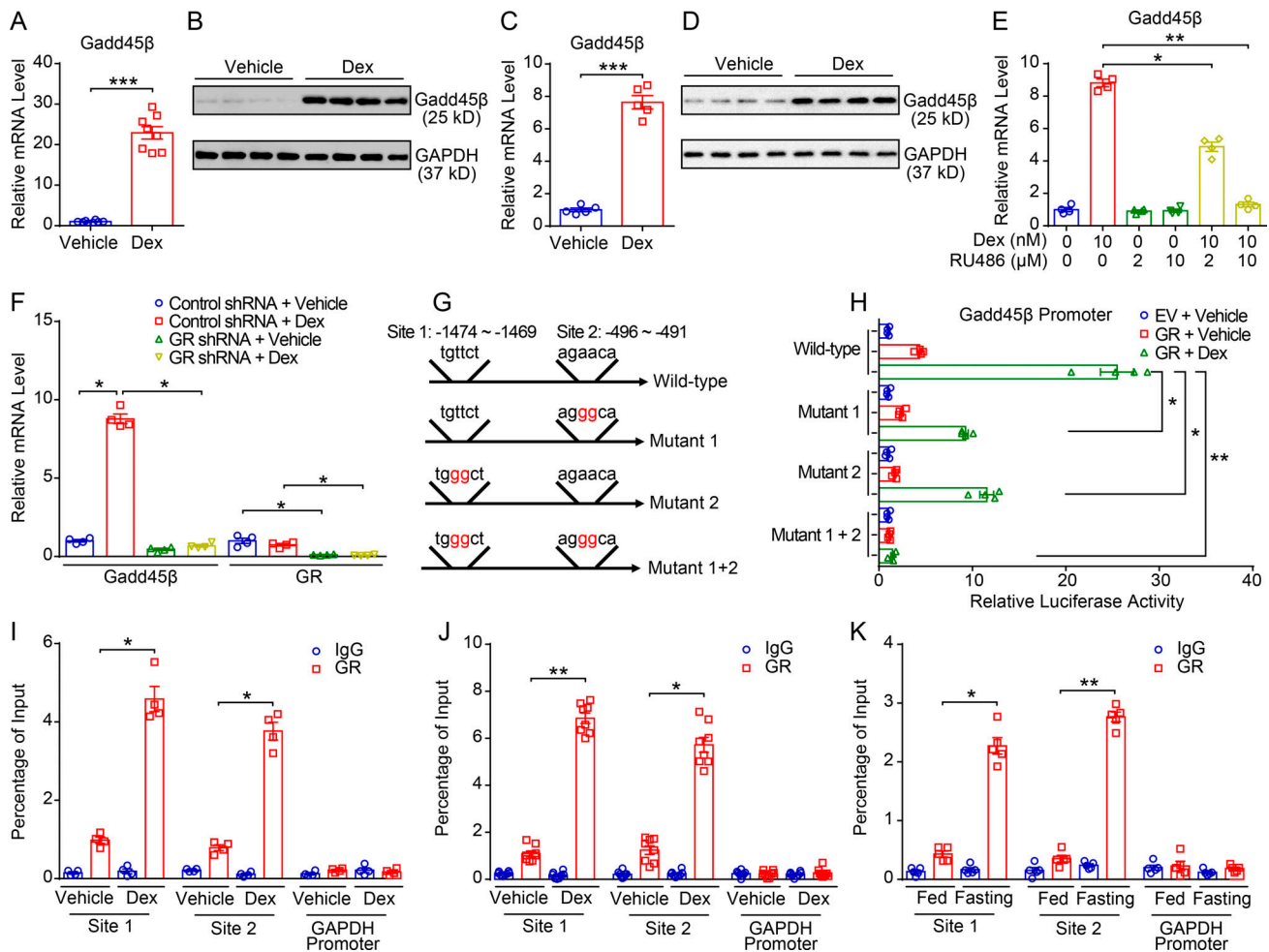


Figure 1. Induction of Gadd45β in the liver by steroid hormone or fasting. (A) Relative mRNA levels of Gadd45β in the livers of C57BL/6 mice treated with Dex (1.0 mg/kg) or vehicle control for 14 d. *n* = 8 per group. (B) Protein levels of hepatic Gadd45β in the two groups of mice described in A. (C) Relative mRNA levels of Gadd45β in MPHs treated with Dex (10 nM) or vehicle control for 12 h. *n* = 5 per group. (D) Protein levels of hepatic Gadd45β in MPHs treated with Dex (10 nM) or vehicle control for 24 h. (E) Relative mRNA levels of Gadd45β in MPHs. Cells were preincubated with RU486 (2 μM or 10 μM) for 4 h, then treated with Dex (10 nM) or vehicle control for another 12 h. *n* = 4 per group. (F) Relative mRNA levels of Gadd45β in MPHs. Cells were transfected with GR shRNA or control shRNA for 24 h, then treated with Dex (10 nM) or vehicle control for another 12 h. *n* = 4 per group. (G) The proximal promoter region of the mouse Gadd45β gene contains two potential half-binding motifs for GR. Mutant sites are highlighted in red. (H) Luciferase reporter assays. HepG2 cells were co-transfected with GR expression plasmids and luciferase reporter plasmids containing wild-type or mutant Gadd45β promoters for 24 h. Then, cells were treated with Dex (10 nM) or vehicle for 12 h before harvest. *n* = 4 in each group. EV, empty vector. (I) ChIP assays showing the association of GR with the two binding sites on the Gadd45β promoter. MPHs were treated with Dex (10 nM) or vehicle control for 1 h and then subjected to ChIP assays. GAPDH proximal promoter was used as a negative control. *n* = 4 per group. (J) ChIP assays showing the association of GR on the Gadd45β promoter in the livers of C57BL/6 mice treated with Dex or vehicle control. *n* = 8 per group. (K) ChIP assays showing the association of GR on the Gadd45β promoter in the livers of C57BL/6 mice under ad libitum–fed, 16-h fasting conditions. *n* = 5 per group. Data are represented as mean ± SEM. *, *P* < 0.05; **, *P* < 0.01; ***, *P* < 0.001. Two-tailed Student's *t* test in A and C; one-way ANOVA in E, F, and H–K. Data are combined from five (C) or four (D–F, H, and I) independent experiments.

shRNA or control shRNA, respectively (Fig. S1 N). Then, we measured the rhythm of plasma GC levels and compared hepatic Gadd45β expression in two groups of mice. Consistent with a previous report (Yang et al., 2006), hepatic GR expression was constant throughout the day and night (Fig. S1 N). A significant diurnal pattern for plasma corticosterone concentrations was observed in two groups of mice (Fig. S1 O). As expected, hepatic Gadd45β mRNA showed a circadian expression similar to that of plasma corticosterone in control shRNA-infected mice (Fig. S1 P, left). However, the basal expression of Gadd45β mRNA was significantly decreased in mice infected with GR shRNA, and the circadian pattern of Gadd45β expression ceased (Fig. S1 P, right).

We further explored the molecular basis of Gadd45β up-regulation by the GC–GR signaling pathway using an online transcription factor scanning system (PROMO software; Messegueur et al., 2002). Bioinformatic analysis showed that the promoter region of the Gadd45β gene, spanning from –2,000 to +1 bp (transcription start site), contains two potential half-glucocorticoid receptor response element (half-GRE) binding sites (Fig. 1 G). When this region was cloned and inserted into a luciferase reporter gene, transfection of a GR expression plasmid activated the luciferase, and this activation was robustly enhanced by Dex treatment (Fig. 1 H). Mutation of the reporter constructs clearly showed that each GRE is functional; mutation

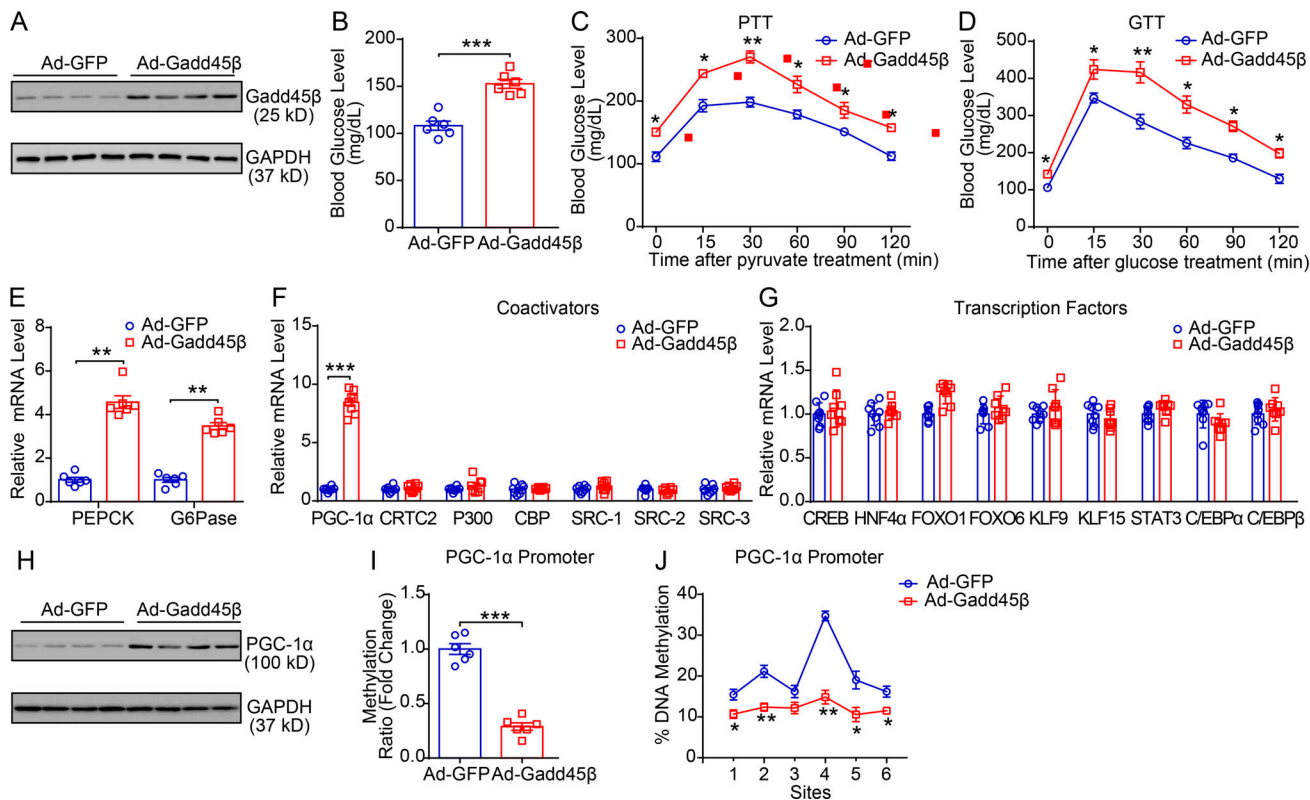


Figure 2. Gadd45β promotes hyperglycemia through DNA demethylation of PGC-1α. (A–J) 2×10^9 PFU per mouse of Ads containing GFP or Gadd45β were delivered into C57BL/6 mice for 15 d. $n = 6$ per group. **(A)** Hepatic Gadd45β protein levels in C57BL/6 mice infected with Ad-Gadd45β or Ad-GFP. **(B)** Blood glucose levels on postinjection day 6. **(C)** PTT on postinjection day 8. **(D)** GTT on postinjection day 11. **(E)** Relative mRNA levels of PEPCK and G6Pase in two groups of mice. **(F and G)** Relative mRNA levels of transcriptional coactivators (F) and transcription factors (G) in the livers of mice infected with Ad-GFP or Ad-Gadd45β. **(H)** PGC-1α protein levels in the livers of C57BL/6 mice infected with Ad-GFP or Ad-Gadd45β. **(I)** Promoter-specific methylation levels were analyzed by MeDIP-qPCR. The ratio of methylated DNA levels in the livers from Ad-GFP- or Ad-Gadd45β-infected mice is presented. **(J)** The percentage of DNA methylation in individual methylated cytosine sites in the livers of Ad-GFP- or Ad-Gadd45β-infected mice was analyzed by pyrosequencing. Data are represented as mean \pm SEM. *, $P < 0.05$; **, $P < 0.01$; ***, $P < 0.001$. Two-tailed Student's *t* test in B, E–G, and I; one-way ANOVA in C, D, and J. Data are representative of two (A–J) independent experiments.

of any site decreased, while mutation of both sites blocked the transactivation role of GCs (Fig. 1 H). A chromatin immunoprecipitation (ChIP) assay further showed that the GR could bind to both sites in MPHs in the presence of Dex (Fig. 1 I). We also confirmed the GC-mediated recruitment of endogenous GR proteins onto the Gadd45β promoter region in the livers of Dex-treated mice and fasted mice (Fig. 1, J and K). Together, these results indicate that GCs up-regulate Gadd45β expression through the GR.

Gadd45β promotes hepatic gluconeogenesis and hyperglycemia in mice

Next, we studied the functions of hepatic Gadd45β in the regulation of glucose metabolism. An adenovirus (Ad) containing Gadd45β (Ad-Gadd45β) was prepared and administered into C57BL/6 mice via tail vein injection (Fig. 2 A). An equal amount of Ad-GFP was used as a control. As a result, blood glucose levels were significantly elevated in fasted mice transfected with Ad-Gadd45β compared with mice transfected with Ad-GFP (Fig. 2 B). The hepatic glycogenolysis and gluconeogenesis pathways are the main sources of endogenous glucose production to maintain blood glucose levels in a fasted state (Rines et al., 2016).

Thus, we first examined the glycogenolysis pathway. No significant difference was detected in the hepatic glycogen content of mice transfected with Ad-Gadd45β versus those transfected with Ad-GFP (Fig. S2 A). In addition, genes related to glycogenolysis were not altered (Fig. S2 B). In contrast, the pyruvate tolerance test (PTT) showed that hepatic gluconeogenesis was enhanced in mice transfected with Ad-Gadd45β (Fig. 2 C). A glucose tolerance test (GTT) indicated that Ad-Gadd45β-infected mice developed impaired glucose tolerance (Fig. 2 D). In agreement, mRNA levels of the gluconeogenic enzymes PEPCK and G6Pase were markedly increased in the livers of Gadd45β-expressing mice (Fig. 2 E).

To further confirm the gluconeogenic effects of Gadd45β in vitro, MPHs were transfected with Ad-Gadd45β or Ad-GFP (Fig. S2 C). Overexpression of Gadd45β promoted cellular glucose production and increased the mRNA levels of gluconeogenic enzymes (Fig. S2, D and E). Thus, Gadd45β appears to function as an important regulator of gluconeogenesis to promote HGP.

Gadd45β promotes the gene expression of PGC-1α

Gadd45β has been shown to activate gene expression by reducing site-specific DNA methylation (Ma et al., 2009; Schüle

et al., 2019). Therefore, to explore the molecular mechanism involved in Gadd45 β regulation of hepatic gluconeogenesis, we performed DNA methylation profiling to analyze the methylomes of livers treated with Dex or vehicle control by methylated DNA immunoprecipitation sequencing (MeDIP-seq). The results showing significant differences in DNA methylation levels are presented as a heatmap (Fig. S2 F). We identified 751 differentially methylated regions (DMRs) between Dex- and vehicle control-treated livers (Fig. S2 G). Strikingly, 394 of these 751 DMRs (52.46%) showed increased methylation levels, while 357 (47.54%) were hypomethylated (Fig. S2 H). To determine whether DMRs correlated with changes in gene expression, we compared MeDIP-seq with RNA-seq, as depicted in Fig. S1 A. This comparison revealed 20 DMR-associated genes that were also differentially expressed (Fig. S2 H). Notably, Ppargc1a, located at chromosome 5, is one of the DMR-associated hypomethylated genes that were up-regulated (Fig. S2, H and I). Ppargc1a encodes a protein called PGC-1 α , a well-established transcriptional coactivator in hepatic gluconeogenesis (Yoon et al., 2001). Therefore, we asked whether PGC-1 α is a downstream target of Gadd45 β in the liver.

Our qRT-PCR analysis confirmed that mRNA levels of PGC-1 α were markedly elevated in the livers of mice transfected with Ad-Gadd45 β (Fig. 2 F), while the expression of other transcriptional coactivators or transcription factors involved in gluconeogenesis, such as CRT2, steroid receptor coactivators, HNF4 α , forkhead box Os, and Krüppel-like factors, remained unchanged (Fig. 2, F and G). The induction of PGC-1 α expression was further confirmed by Western blotting analysis (Fig. 2 H). Overexpression of Gadd45 β also increased PGC-1 α mRNA and protein expression in MPHs (Fig. S2, J and K). To determine whether the gluconeogenic effects of Gadd45 β were PGC-1 α dependent, an Ad encoding an shRNA targeting PGC-1 α was generated and transfected into MPHs (Fig. S2 L). Knockdown of endogenous PGC-1 α significantly attenuated the effects of Gadd45 β to induce the expression of PEPCK and G6Pase (Fig. S2). Consistently, enhanced cellular glucose production by Gadd45 β was also largely blocked by depletion of PGC-1 α (Fig. S2 M). Thus, we can conclude that PGC-1 α is essential for the gluconeogenic functions of Gadd45 β in hepatocytes.

Gadd45 β induces the expression of PGC-1 α by removing DNA methylation at the promoter region

Next, we examined whether the induction of PGC-1 α expression by Gadd45 β can be attributed to changes in DNA methylation. Previous studies have demonstrated that cytosine hypermethylation levels of the PGC-1 α promoter were negatively correlated with the mRNA expression and biological functions of PGC-1 α (Barrès et al., 2009; Barrès et al., 2012; Laker et al., 2014). This promoter region spans -360 to -60 bp relative to the transcription start site and contains several methylation sites; one major locus is located within the CREB binding site (Fig. S3 A), the most important cis-regulatory element for PGC-1 α transcription (Herzig et al., 2001). Our ChIP assays showed that Gadd45 β can occupy the PGC-1 α promoter region in MPHs, which was enhanced by Dex treatment (Fig. S3 B). Through

methylated DNA immunoprecipitation (MeDIP) followed by qRT-PCR (MeDIP-qPCR) and pyrosequencing analysis, we found that the methylation status of the PGC-1 α promoter was significantly reduced in the livers of mice infected with Ad-Gadd45 β (Fig. 2, I and J). This reduction was also observed in MPHs overexpressing Gadd45 β (Fig. S3, C and D). However, global DNA methylation levels were not altered by Gadd45 β expression (Fig. S3, E and F). In addition, the methylation status at the promoter region of Dhx15, a gene adjacent to PGC-1 α on chromosome 5, remained unaffected in the livers of mice or MPHs overexpressing Gadd45 β (Fig. S3, G and H). These results confirm that Gadd45 β regulates DNA methylation patterns at specific gene loci. Moreover, Gadd45 β did not increase the cytosine methylation of the PEPCK or G6Pase promoter regions in mouse livers or MPHs (Fig. S3, I-L), indicating that Gadd45 β indirectly up-regulates their gene expression. In agreement with the gluconeogenic role of Gadd45 β , the reduced DNA methylation pattern in the PGC-1 α promoter was also found in the livers of Dex-treated or fasted mice (Fig. S3, M-P).

Changes in DNA methylation status usually affect the binding affinity of specific transcription factors and histones, leading to altered gene transcription (Martínez et al., 2014). Using ChIP assays, we found that the interaction of phosphorylated CREB with the PGC-1 α promoter, which was activated by cAMP signaling, was dramatically increased when Gadd45 β was overexpressed in MPHs (Fig. S3 Q). In addition, we observed a reduction in repressive histones (histone H3 lysine 9 trimethylation [H3K9me3] and H3K27me3) and an enrichment in active histones (H3K4me3) in the PGC-1 α promoter in MPHs overexpressing Gadd45 β (Fig. S3 R). Together, these data indicate that a reduced DNA methylation status caused by Gadd45 β at the PGC-1 α promoter region is likely associated with enhanced CREB binding and active histone modifications, resulting in the up-regulation of PGC-1 α expression. Therefore, our results also well explained why GCs had a synergistic effect with cAMP signaling to activate PGC-1 α expression (Yoon et al., 2001).

Gadd45 β promotes DNA demethylation of PGC-1 α in conjunction with ten-eleven translocation 1 (TET1)

Previous studies have shown that TET methylcytosine dioxygenase is responsible for converting 5-methylcytosine (5mC) sequentially to 5-hydroxymethylcytosine (5hmC), 5-formylcytosine, 5-carboxylcytosine, and unmethylated cytosine (Wu and Zhang, 2017). Therefore, we determined the molecular basis in Gadd45 β -mediated active demethylation and activation of the PGC-1 α gene. Using ChIP assays, we observed a considerable occupancy of TET1, but not TET2 or TET3, at the PGC-1 α promoter in the MPHs overexpressing Gadd45 β (Fig. 3 A), which was associated with an increment of DNA 5hmC (Fig. 3 B). Consistently, Dex stimulation dramatically increased TET1 binding to the PGC-1 α promoter, resulting in increased 5hmC at its promoter (Fig. 3, C and D). Coimmunoprecipitation experiments further showed that there is a direct protein-protein interaction between Gadd45 β and TET1 in MPHs (Fig. 3 E). Besides, compared with Gadd45 β alone, cotransfection of TET1 with Gadd45 β further reduced DNA methylation status at the PGC-1 α promoter (Fig. 3, F and G), leading to enhanced expression of PGC-1 α and gluconeogenic enzymes (Fig. 3 H). Cellular glucose

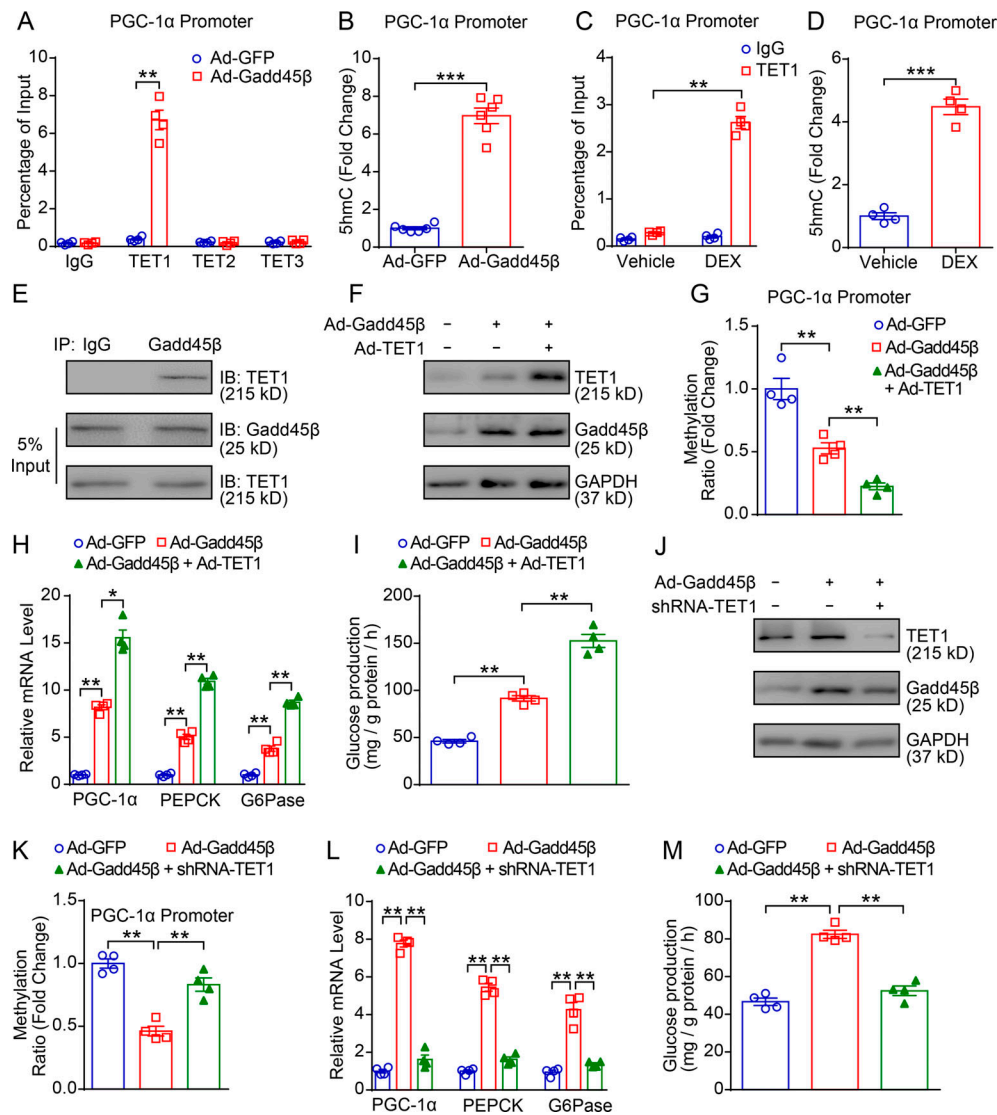


Figure 3. Gadd45 β promotes PGC-1 α expression in conjunction with TET1. (A) ChIP-qPCR assays showing the occupancy of TET1 at the PGC-1 α promoter in MPHs transfected with Ad-GFP or Ad-Gadd45 β . $n = 4$ per group. (B) DNA 5-hydroxymethylation was measured in the promoter region of the PGC-1 α gene in MPHs transfected with Ad-GFP or Ad-Gadd45 β . $n = 6$ per group. (C) ChIP-qPCR assays showing the occupancy of TET1 at the PGC-1 α promoter in MPHs treated with Dex or vehicle control. $n = 4$ per group. (D) DNA 5-hydroxymethylation was measured in the promoter region of the PGC-1 α gene in MPHs treated with Dex or vehicle control. $n = 4$ per group. (E) Protein-protein interaction between Gadd45 β and TET1. Gadd45 β was immunoprecipitated (IP) from MPHs, followed by Western blot (IB) to detect TET1. (F) Protein expression of Gadd45 β or TET1 in MPHs transfected with Ad as indicated. (G) Promoter-specific methylation levels were analyzed by MeDIP-qPCR. The ratio of methylated DNA levels in MPHs infected with Ad-GFP, Ad-Gadd45 β , or Ad-Gadd45 β plus Ad-TET1 is presented. $n = 4$ per group. (H and I) Relative mRNA levels of gluconeogenic genes (H) and cellular glucose production (I) in MPHs as described in F. (J) Protein expression of Gadd45 β or TET1 in MPHs transfected with Ad or shRNA as indicated. (K) Promoter-specific methylation levels were analyzed by MeDIP-qPCR. The ratio of methylated DNA levels in MPHs infected with Ad-GFP, Ad-Gadd45 β , or Ad-Gadd45 β plus shRNA-TET1 is presented. $n = 4$ per group. (L and M) Relative mRNA levels of gluconeogenic genes (L) and cellular glucose production (M) in MPHs as described in J. Data are represented as mean \pm SEM. *, $P < 0.05$; **, $P < 0.01$; ***, $P < 0.001$. Two-tailed Student's t test in A, B, and D; one-way ANOVA in C, G-I, and K-M. Data are representative of or combined from three (E, F, and J) or four (A-D, G-I, and K-M) independent experiments.

production was also increased by combination of TET1 with Gadd45 β (Fig. 3 I), suggesting a functional cooperation of Gadd45 β and TET1. On the other hand, knockdown of endogenous TET1 expression impaired Gadd45 β -induced DNA demethylation (Fig. 3, J and K) and reversed Gadd45 β -mediated gluconeogenic effects (Fig. 3, L and M). These results indicate that Gadd45 β acts as a bridging protein between TET1 and methylated DNA at the PGC-1 α promoter region, while TET1-associated DNA demethylation might be crucial for the transcriptional activation of the PGC-1 α gene.

Hepatic Gadd45 β -deficient mice have an improved glucose metabolism

To further examine the metabolic function of Gadd45 β in vivo, two loxP sites were inserted into the Gadd45 β gene flanking exons 1–4 to generate Gadd45 β flox/flox (F/F) mice (Fig. S4 A). We then obtained liver-specific Gadd45 β -knockout mice (LKO mice) by injection of adeno-associated virus (AAV)-expressing Cre or GFP recombinase into Gadd45 β F/F mice through the tail vein. The AAV approach was chosen in our study because (1)

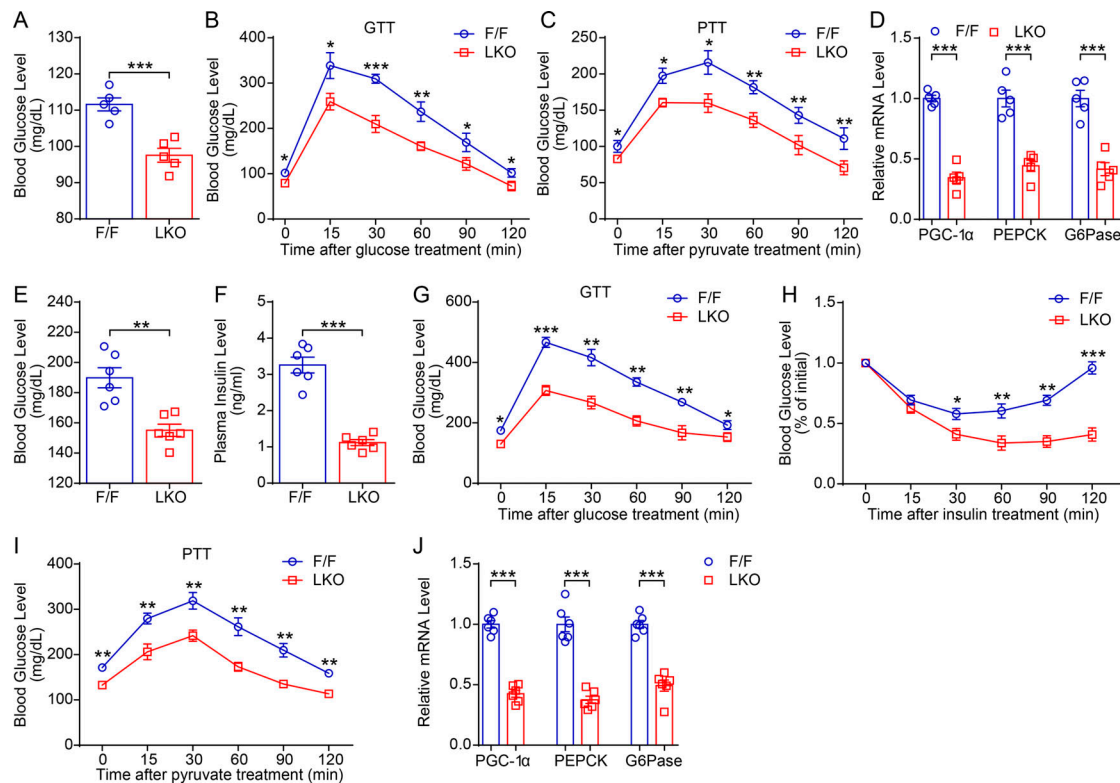


Figure 4. Gadd45 β LKO mice had an improved glucose metabolism. (A–D) Glucose metabolism in Gadd45 β F/F and LKO males fed a normal diet. $n = 5$ per group. **(A)** Fasting blood glucose levels. **(B)** GTT. **(C)** PTT. **(D)** mRNA expression of gluconeogenic genes. **(E–J)** Glucose metabolism in Gadd45 β F/F and LKO males fed an HFD for 12 wk. $n = 6$ per group. **(E)** Fasting blood glucose levels. **(F)** Fasting blood insulin levels. **(G)** GTT. **(H)** ITT. **(I)** PTT. **(J)** mRNA expression of gluconeogenic genes. Data are represented as mean \pm SEM. *, $P < 0.05$; **, $P < 0.01$; ***, $P < 0.001$. Two-tailed Student's t test in A, D–F, and J; one-way ANOVA in B, C, and G–I. Data are representative of two (A–J) independent experiments.

AAV-mediated gene transduction did not induce immune responses and toxicity in mice; (2) the Cre or GFP recombinase expression was driven by the liver-specific thyroxine binding globulin promoter; (3) it can persistently be expressed in the liver for >20 wk (Liu et al., 2016; Yazdanyar et al., 2013); and (4) we could carry out this experiment in adult mice to avoid perturbing the proliferation or differentiation of hepatocytes at the developmental stage. Our qRT-PCR and Western blotting analyses confirmed that Gadd45 β expression was substantially and specifically reduced in the livers of LKO mice, while its expression was unaffected in other tissues examined (Fig. S4, B and C). No differences were found in body weight, body length, food intake, and percentage of fat mass between Gadd45 β LKO and F/F mice (data not shown).

Notably, the fasting glucose levels were significantly decreased in Gadd45 β LKO mice (Fig. 4 A). We also found that Gadd45 β LKO mice had a greater glucose tolerance compared with F/F mice (Fig. 4 B). HGP, determined by PTT, was lower in LKO than in F/F mice (Fig. 4 C). The lower blood glucose levels in LKO animals are due to impaired gluconeogenesis, as reflected in the reduced expression of PGC-1 α and gluconeogenic enzymes (Fig. 4 D). Levels of plasma insulin, glucagon, corticosterone, and liver injury markers (alanine aminotransferase and aspartate aminotransferase) were unchanged (Fig. S4 D).

We then fed two groups of mice a high-fat diet (HFD) for 12 wk, which can induce hyperglycemia and glucose intolerance.

Depletion of hepatic Gadd45 β in mice did not alter body weight gain; however, LKO mice had a significantly improved glucose metabolism, as shown by reduced fasting blood glucose concentrations (Fig. 4 E). Mice without hepatic Gadd45 β also had lower basal blood insulin levels (Fig. 4 F), suggesting insulin hypersensitivity in these mice. Consistently, LKO mice showed markedly improved glucose and insulin tolerance (Fig. 4, G and H). HGP was also lower in the LKO mice than in the F/F mice (Fig. 4 I). In addition, expression levels of gluconeogenic genes were lower in the livers of LKO mice (Fig. 4 J). Thus, these data indicate that liver-specific suppression of Gadd45 β could prevent dietary obesity-induced metabolic impairment independently of changes in body weight.

Gadd45 β LKO mice are resistant to Dex-induced hyperglycemia

Based on the above results, we speculate that hepatic Gadd45 β might also be required for steroid-induced hyperglycemia. To test this hypothesis *in vivo*, we treated Gadd45 β LKO and F/F mice with Dex or vehicle control for 14 d. Body weights and food intake were comparable between each subgroup (Fig. S4, E and F). Dex treatment led to hyperglycemia in Gadd45 β F/F mice (Fig. 5 A, column 2 versus column 1), but not in Gadd45 β LKO mice (Fig. 5 A, column 4 versus column 3). Moreover, Dex-induced HGP and glucose intolerance were largely abrogated by hepatic Gadd45 β deficiency (Fig. 5, B–E). Thus, ablation of

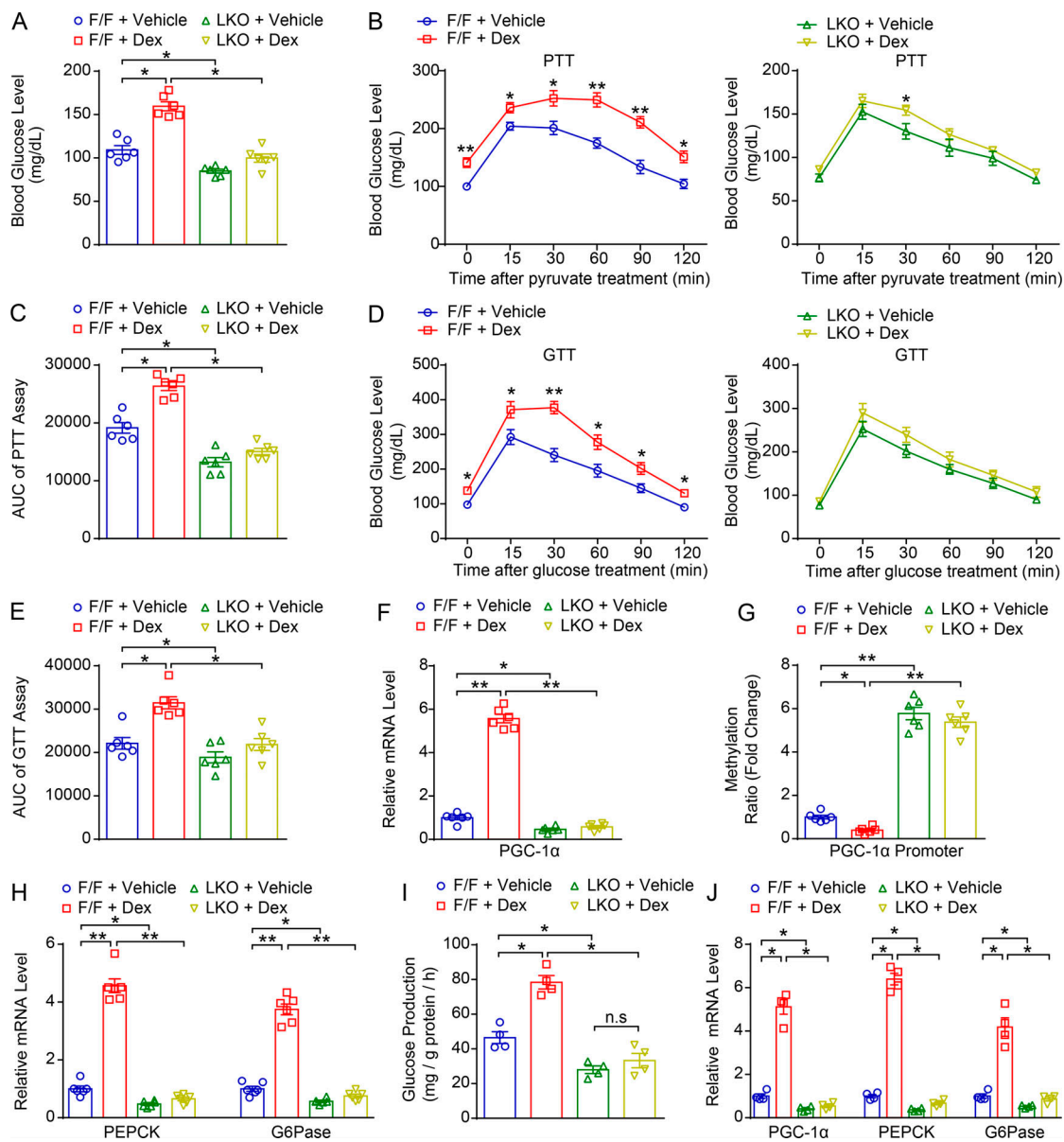


Figure 5. **Gadd45 β LKO mice are resistant to Dex-induced hyperglycemia.** (A–H) Gadd45 β F/F or LKO mice were treated with Dex (1.0 mg/kg) or vehicle control for 14 d. *n* = 6 per group. (A) Blood glucose levels in 16-h fasted Gadd45 β F/F or LKO mice at day 12. (B and C) PTT (B) and the corresponding area under the curve (AUC; C) at day 6. (D and E) GTT (D) and the corresponding AUC (E) at day 9. (F) Relative mRNA levels of PGC-1 α in the livers of mice. (G) Promoter-specific methylation levels at the PGC-1 α promoter region were analyzed by MeDIP-qPCR. (H) Relative mRNA levels of PEPCK and G6Pase in the liver. (I) Glucose production in MPHs isolated from Gadd45 β F/F or LKO mice in the presence of Dex (10 nM) or vehicle control. *n* = 4 per group. (J) Relative mRNA levels of PGC-1 α , PEPCK, and G6Pase in MPHs from Gadd45 β F/F or LKO mice in the presence of Dex (10 nM) or vehicle control. *n* = 4 per group. *, *P* < 0.05; **, *P* < 0.01. One-way ANOVA (A–J). Data are representative of or combined from two (A–H) or four (I and J) independent experiments.

Gadd45 β in the liver can protect against Dex-associated hyperglycemia. Consistent with this notion, we found that Dex treatment can induce the expression of PGC-1 α due to decreased DNA methylation at its promoter region in Gadd45 β F/F mice, but not in LKO mice (Fig. 5, F and G). Additionally, induction of PEPCK and G6Pase by Dex was also defective in Gadd45 β LKO mice (Fig. 5 H).

To confirm these findings in an independent setting, MPHs were isolated from the livers of Gadd45 β F/F and LKO mice, followed by incubation with Dex or vehicle control. In agreement with the *in vivo* observations, Dex treatment of MPHs from Gadd45 β F/F mice resulted in a significant elevation in

cellular glucose production and gluconeogenic gene expression (Fig. 5, I and J, column 2 versus column 1). However, these effects were blocked in MPHs from Gadd45 β LKO mice (Fig. 5, I and J, column 4 versus column 3). Collectively, our data clearly demonstrate the essential role of Gadd45 β in mediating steroid-induced hyperglycemia and hepatic gluconeogenesis.

Up-regulation of hepatic Gadd45 β in diabetic mice and human subjects

It has been established that enhanced hepatic gluconeogenesis is a major contributor to hyperglycemia in diabetic patients

(Petersen et al., 2017; Rines et al., 2016). Therefore, we speculate that Gadd45 β expression would be dysregulated in the livers of diabetic mice. To test it, leptin receptor-deficient *db/db* mice, leptin-deficient *ob/ob* mice, and C57BL/6 mice fed an HFD for 12 wk were used. Plasma corticosterone levels are usually higher in *db/db* and *ob/ob* mice, compared with normal lean mice (Liu et al., 2003; Liu et al., 2005; Liu et al., 2006). Besides, while no significant differences in circulating corticosterone concentration between mice fed an HFD and normal chow diet, hepatic GR signaling or sensitivity was enhanced in the livers of HFD-induced obese mice (Quagliarini et al., 2019; Dassonville et al., 2020). As expected, these mice displayed hyperglycemia and insulin resistance, which were described in our previous study (Lu et al., 2014). The expression of several gluconeogenic genes, including PGC-1 α , PEPCK, and G6Pase, was significantly increased in the livers of these mice compared with their corresponding control mice (Fig. S4, G–I). Furthermore, qRT-PCR and Western blot analysis showed that hepatic Gadd45 β expression levels were significantly up-regulated in *db/db* mice compared with lean controls (Fig. 6, A and B). Similar results were observed in *ob/ob* mice and HFD mice (Fig. 6, C–F). Besides, either RU486 treatment or GR shRNA infection led to a decreased expression of Gadd45 β in the livers of HFD-induced obese mice, indicative of the important role of GC–GR signaling in the regulation of HFD-associated hepatic Gadd45 β expression (Fig. S4, J–M). Consistent with these findings, we found that the DNA methylation status was reduced at the PGC-1 α promoter in all three types of obese mice (Fig. S4, N–P).

In addition, we obtained human liver samples from patients with T2DM and from nondiabetic normal individuals through ultrasonography-guided percutaneous needle liver biopsies. qRT-PCR analysis showed that expression levels of Gadd45 β , PGC-1 α , and gluconeogenic enzymes (PEPCK and G6Pase) were up-regulated in diabetic patients compared with normal subjects (Fig. 6 G). Moreover, there was a positive correlation between Gadd45 β mRNA levels and both fasting plasma glucose and hemoglobin A1c (HbA1c) levels (Fig. 6, H and I). A significant correlation between mRNA levels of Gadd45 β and gluconeogenic genes was also observed (Fig. S4, Q–S). Thus, these results indicate that elevated hepatic Gadd45 β expression is associated with the development of hyperglycemia in T2DM.

Knockdown of hepatic Gadd45 β improves hyperglycemia and glucose intolerance in diabetic mice

The dysregulation of hepatic Gadd45 β in diabetic mice and human subjects prompted us to investigate whether its deficiency could improve glucose homeostasis. We transfected *db/db* mice with Gadd45 β -specific adenoviral shRNA via the tail vein, which inhibited endogenous Gadd45 β expression in the liver (Fig. 7 A). The reduction of Gadd45 β caused a marked increase in DNA methylation status of the PGC-1 α promoter (Fig. 7, B and C), subsequently leading to its down-regulation (Fig. 7, D and E). In agreement, expression levels of PEPCK and G6Pase were reduced (Fig. 7 F). Compared with negative controls, knockdown of Gadd45 β alleviated hyperglycemia and hyperinsulinemia in *db/db* mice (Fig. 7, G and H), although body weight and food intake remained unchanged (data not shown). In *db/db* mice

with Gadd45 β deficiency, PTT and GTT results showed a decrease in gluconeogenesis and an improvement in glucose tolerance, respectively (Fig. 7, I and J). Moreover, insulin sensitivity was enhanced, as evidenced by the results of insulin tolerance tests (ITTs; Fig. 7 K). The beneficial effects on glucose metabolism were also observed in HFD-induced obese mice. Knockdown of Gadd45 β in the livers of HFD mice also reduced the expression of PGC-1 α and gluconeogenic enzymes due to hypermethylation at the PGC-1 α promoter (data not shown). Furthermore, diabetes-associated metabolic syndromes, including hyperglycemia, hyperinsulinemia, glucose intolerance, and insulin resistance, were alleviated (data not shown).

In summary, our results demonstrated that, upon binding of GCs such as cortisol and Dex, GR up-regulates the expression of Gadd45 β , which in turn activates PGC-1 α gene transcription through DNA demethylation at its promoter region. PGC-1 α can further induce the expression of gluconeogenic genes to enhance hepatic gluconeogenesis and glucose production (Fig. 8), leading to hyperglycemia, glucose intolerance, and diabetes.

Discussion

In the present study, through RNA-seq analysis of two mouse models, we identified Gadd45 β as an important potentiating epigenetic factor that activates hepatic gluconeogenesis to enhance HGP. Ad-mediated overexpression of Gadd45 β enhanced gluconeogenesis and glucose production in vivo and in primary hepatocytes. In contrast, Gadd45 β LKO mice not only showed hypoglycemia in a fasted state, but they were also resistant to HFD-induced and Dex-associated glucose intolerance. Therefore, our findings might be of both physiological and pathophysiological interest, as Gadd45 β expression can be induced by starvation, steroid use, and obesity.

Methylation of the PGC-1 α promoter can be regulated in skeletal muscle in response to proinflammatory cytokines or free fatty acids through the actions of DNA methyltransferase 3B (Barrès et al., 2009). However, whether the methylation status of PGC-1 α promoter is dynamically regulated in the liver remains elusive. Here, we show that fasting, steroid use, and obesity can reduce the methylation at the PGC-1 α promoter through the actions of Gadd45 β , a member of a small gene family that also includes Gadd45 α and Gadd45 γ . This family was originally identified as a group of growth-suppressing genes that induce cell cycle arrest and apoptosis (Schäfer, 2013). However, alterations of hepatic Gadd45 β activity caused little change in the expression levels of cell cycle-related genes (data not shown). Besides, there were no significant differences in terminal deoxynucleotidyl transferase dUTP nick end labeling incorporation assays in the livers of mice with hepatic Gadd45 β overexpression or depletion (data not shown). Of note, all of the in vivo experiments in this study, including overexpression, depletion, and knockdown of Gadd45 β , were performed in the livers of adult mice. Therefore, our findings suggest that the metabolic role of Gadd45 β in quiescent tissues, such as the liver, might be independent of cell proliferation, apoptosis, or differentiation. Consistent with this notion, recent studies demonstrated that components of the cell cycle machinery like Cyclin

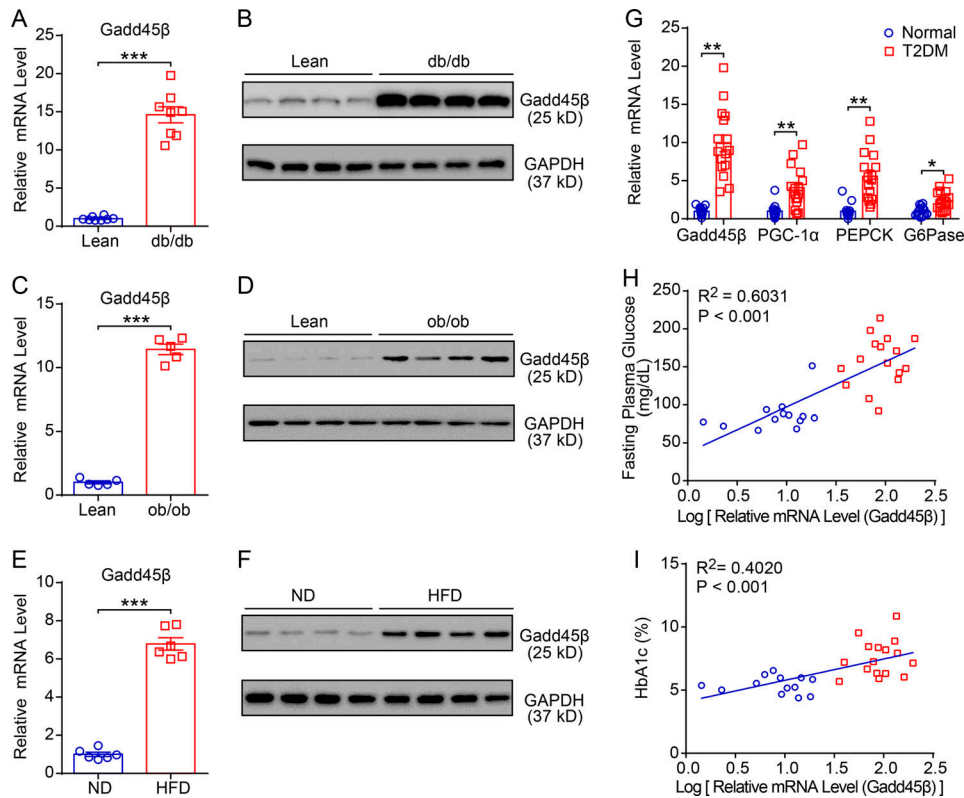


Figure 6. **Hepatic Gadd45β expression is elevated in diabetic mice and human subjects.** (A and B) mRNA expression levels (A) and protein contents (B) of hepatic Gadd45β in *db/db* and lean mice. *n* = 8 per group. (C and D) mRNA expression levels (C) and protein contents (D) of hepatic Gadd45β in *ob/ob* and lean mice. *n* = 5 per group. (E and F) mRNA expression levels (E) and protein contents (F) of hepatic Gadd45β in C57BL/6 mice fed a normal diet (ND) or HFD for 12 wk. *n* = 6 per group. (G) Relative mRNA expression of Gadd45β, PGC-1α, PEPCCK, and G6Pase in livers from normal subjects (*n* = 13) and patients with T2DM (*n* = 16). (H and I) Pearson correlation analysis for normalized Gadd45β mRNA levels versus fasting plasma glucose (H) and HbA1c levels (I) in human subjects (*n* = 29). Blue circle, normal; red square, T2DM. *, *P* < 0.05; **, *P* < 0.01; ***, *P* < 0.001. Two-tailed Student's *t* test (A, C, E, and G); Pearson correlation analysis (H and I). Data are representative of two (A–F) independent experiments.

D1-CDK4 could control hepatic glucose homeostasis independently of cell division (Lee et al., 2014; Bhalla et al., 2014). Indeed, emerging studies have revealed the diverse functions of the Gadd45 family in various biological systems via active DNA demethylation of specific gene loci (Schäfer, 2013). Gadd45-mediated DNA demethylation is usually initiated by cellular stimuli and is accompanied by simultaneous Gadd45 family gene induction. For instance, Gadd45α was selectively up-regulated during the osteogenic differentiation of mesenchymal stem cells to demethylate key osteogenic genes, like Runx2 and Dlx5 (Zhang et al., 2011). In addition, Gadd45β expression was rapidly induced by neuronal activity, which is essential for the DNA demethylation of specific promoters and the expression of genes for adult neurogenesis, like BDNF and FGF-1 (Ma et al., 2009). These findings indicate that Gadd45 proteins may represent an important nexus linking physiological or pathological stimuli to epigenetic DNA modification and gene expression. While Gadd45 proteins lack enzymatic activity, it is nowadays believed that Gadd45α and Gadd45β contribute to demethylation in conjunction with other modifiers, such as TET or thymine DNA glycosylase (TDG; Schüle, et al., 2019; Bayraktar and Kreutz, 2018; Li et al., 2015). This interaction enhances TET or TDG activity, possibly by tethering them to specific sites of DNA

demethylation. Therefore, together with these studies, our results support the notion that Gadd45β could be an adaptor protein that enhances turnover of DNA methylation. Nevertheless, the precise mechanism(s) contributing to demethylation at specific genomic sites warrants more detailed investigation. Questions remain, such as how is the Gadd45β specifically targeted to the PGC-1α promoter? Are other DNA demethylation machineries, such as TDG protein, also involved in hepatic gluconeogenesis and hyperglycemia?

In addition to the regulation of hepatic gluconeogenesis, PGC-1α acts as a critical switch for multiple biological functions in the liver, including insulin sensitivity and fatty acid oxidation (Lin et al., 2005; Piccinin et al., 2019). PGC-1α has been shown to promote insulin resistance through PPARα-dependent induction of tribbles homolog 3 (TRB3), which inactivates AKT to disrupt insulin signaling (Koo et al., 2004). Here, we showed that Gadd45β is up-regulated in the liver of diabetic mice and patients. Besides, liver-specific Gadd45β-deficient mice are resistant to HFD-induced insulin resistance and hyperinsulinemia. Moreover, knockdown of hepatic Gadd45β increased insulin sensitivity and reduced plasma insulin concentrations in *db/db* mice and HFD-induced obese mice. Consistently, we found that TRB3 expression was up-regulated, while insulin-stimulated

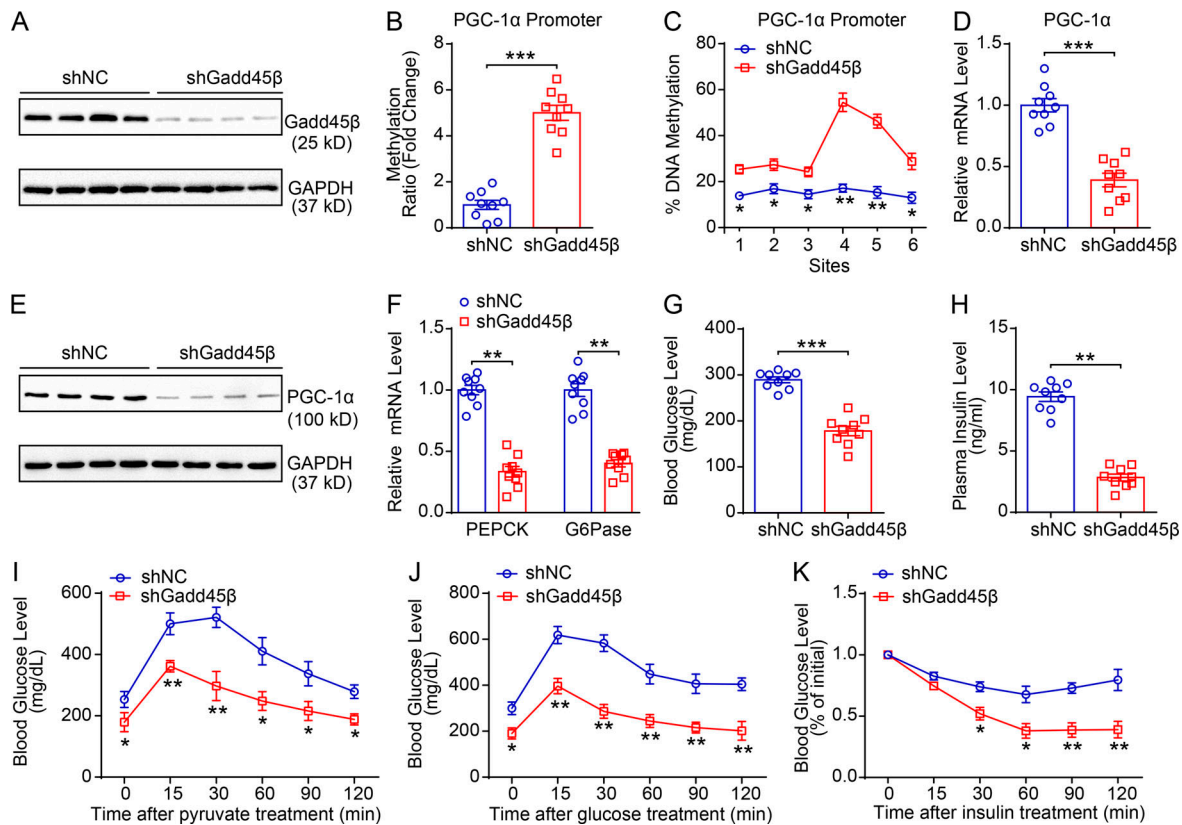


Figure 7. Hepatic Gadd45β knockdown reduces gluconeogenesis and improves hyperglycemia in *db/db* mice. (A–K) 10-wk-old *db/db* mice were injected with adenoviral shRNA targeting Gadd45β (shGadd45β) or negative control (shNC) via the tail vein. (A) Protein levels of Gadd45β in the liver on postinjection day 14. (B) Promoter-specific methylation levels at the PGC-1α promoter region were analyzed by MeDIP-qPCR. (C) The percentage of DNA methylation in individual methylated cytosine sites in livers. (D and E) mRNA and protein expression levels of hepatic PGC-1α. (F) Relative mRNA levels of PEPCK and G6Pase. (G) Blood glucose levels in 16-h fasted mice at day 12. (H) Plasma insulin levels at day 14. (I–K) PTTs (I), GTTs (J), and ITTs (K) performed in the two groups of mice. Data are represented as mean ± SEM. *, P < 0.05; **, P < 0.01; ***, P < 0.001. Two-tailed Student's *t* test (B, D, and F–H). One-way ANOVA (C and I–K). Data are representative of two (A–K) independent experiments.

phosphorylated AKT and GSK3β were reduced, in the livers of mice with hepatic Gadd45β overexpression (Fig. S5, A and B). Therefore, we speculate that Gadd45β might impair insulin sensitivity through a PGC-1α/TRB3/AKT-dependent pathway.

In addition, PGC-1α was shown to coactivate PPARα to enhance the expression of genes involved in fatty acid oxidation and ketogenesis. As a result, mice lacking PGC-1α displayed fasting-induced liver steatosis (Leone et al., 2005). Similarly, increased triglyceride (TG) contents were observed in our Gadd45β LKO mice in the fasted state (Fig. S5 C), at least in part due to reduced expression of PPARα target genes and impaired fatty acid oxidation (Fig. S5, D and E). In agreement, expression of these genes was induced in the livers of mice overexpressing Gadd45β, resulting in a lower hepatic TG content (Fig. S5, F–H). To evaluate the possibility that TET1 might be also involved in the Gadd45β-associated hepatic TG metabolism, we introduced Gadd45β in the liver while simultaneously depleting TET1 with an Ad that expresses TET1-targeting shRNA in C57BL/6 mice (Fig. S5 I). As expected, knockdown of TET1 largely abolished the effects of Gadd45β in lowering TG contents and induction of fatty acid oxidation-related genes (Fig. S5, J–L). Besides, to confirm that the decrease in PGC-1α contributes to hepatic TG accumulation observed in Gadd45β LKO mice, we performed

PGC-1α rescue in livers of Gadd45β LKO mice (Fig. S5 M). As a result, restoration of PGC-1α could alleviate the fasting-associated lipid accumulation by hepatic Gadd45β deficiency (Fig. S5 N). PGC-1α overexpression also reversed the decreased expression of fatty acid oxidation-related genes and plasma β-hydroxybutyrate concentrations (Fig. S5, O and P). On the other hand, while TRB3 is down-regulated in the livers of Gadd45β LKO mice, its restoration cannot rescue the phenotypes of lipid metabolism in Gadd45β LKO mice (Fig. S5, Q–T). Collectively, our results showed that the role of Gadd45β in the regulation of hepatic lipid metabolism could be, at least in part, through TET1 and PGC-1α, suggesting that the functions of Gadd45β and PGC-1α in hepatic glucose and lipid metabolism may partially overlap (Fig. S5 U).

In prolonged fasting, elevated GCs have been shown to inhibit fatty acid synthesis through repression of SREBP-1c (Roqueta-Rivera et al., 2016) while promoting fatty acid oxidation through up-regulation of PGC-1α, PPARα, and FGF21 (Goldstein and Hager, 2015). This might be important for fuel production during fasting. Especially, activation of fatty acid oxidation is required for the endergonic steps of gluconeogenesis for the supply of ATP and nicotinamide adenine dinucleotide plus hydrogen, as both pathways are partially localized in

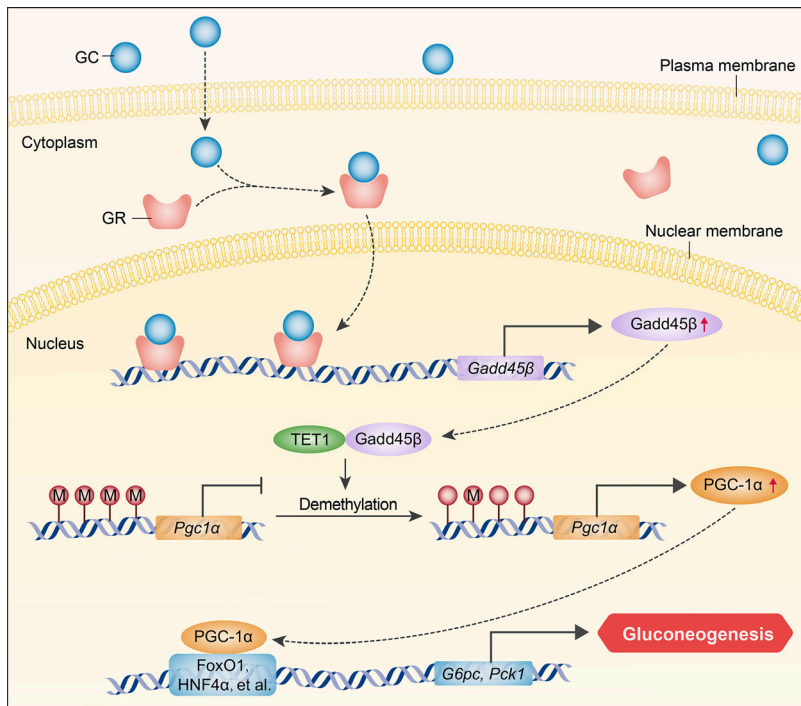


Figure 8. **Working model.** Upon binding of GCs, GR up-regulates the expression of Gadd45 β , which interacts with TET1 to activate PGC-1 α gene transcription through DNA demethylation at its promoter region. PGC-1 α can further induce the expression of gluconeogenic genes to enhance hepatic gluconeogenesis and glucose production. M, DNA methylation.

liver mitochondria (Goldstein and Hager, 2015). For instance, PGC-1 α -, PPAR α -, or FGF21-null mice subjected to prolonged fasting develop fatty liver accompanied with severely hypoglycemia, at least in part due to defects in fatty acid oxidation (Leone et al., 2005; Kersten et al., 1999; Liang et al., 2014), which is similar to our observations in Gadd45 β LKO mice. On the other hand, human studies showed that there was a strong correlation between TCA cycle flux and PEPCK (Sunny et al., 2011), consistent with the induction of gluconeogenesis by fat oxidation (Chen et al., 1999; Roden et al., 2000; Staehr et al., 2003). Therefore, we speculate that up-regulation of Gadd45 β by fasting GC response may mediate several metabolic adaptation responses to starvation, including hepatic gluconeogenesis and fatty acid oxidation. Moreover, our findings also support the notion that hepatic steatosis under certain conditions can be dissociated from glucose intolerance and insulin resistance, which have been reported in recent genetic mouse models and clinical studies (Sun and Lazar, 2013).

Additionally, global Gadd45 β -KO mice generated by Fuhrmeister et al. (2016) showed no obvious changes in blood glucose levels under normal diet but impaired glucose homeostasis under an HFD. Although the reasons behind these conflicting data remain unclear, one possibility is that Gadd45 β is also highly expressed in other metabolic organs/tissues beyond the liver, including adipose tissue, skeletal muscle, and the pancreatic islet (Solomon et al., 2010; Chadwick et al., 2015; Larsen et al., 2006). These observations suggest that the global Gadd45 β deficiency might be insufficient to explore the hepatic role of Gadd45 β in glucose homeostasis, as distinct phenotypes between global KOs and LKOs have been shown in many reports (Koo et al., 2004; Yu et al., 2015; Okamoto et al., 2007). Therefore, the liver-specific role of Gadd45 β in the regulation of glucose metabolism is a question of interest and needs to be

elucidated. To address this issue, multiple strategies were employed in our current study, including LKO mice, Ad-mediated hepatic overexpression and knockdown, and in vitro studies performed in MPHs, which, in our opinion, might be sufficient to explore the liver-specific functions of Gadd45 β in glucose homeostasis. Indeed, all of our data consistently demonstrated that Gadd45 β in the liver acts as an important checkpoint to respond to hormonal stimuli, which in turn activate a gluconeogenic program to induce hyperglycemia and glucose intolerance.

In conclusion, we propose that activation of the Gadd45 β -mediated epigenetic effects represent a novel mechanism underlying hyperglycemia and diabetes. Inhibition of gluconeogenesis and HGP has been used as an effective strategy to screen novel antidiabetic drugs (Rines et al., 2016). Especially, compounds that selectively inhibit the hepatic gluconeogenic role of PGC-1 α have been shown to possess a glucose-lowering effect in a preclinical diabetic mouse model (Sharabi et al., 2017). In addition, circulating GC concentrations are elevated in genetically diabetic mice (e.g., *db/db*, *ob/ob* mice), and elevated plasma cortisol levels have also been observed in diabetic patients or subjects with glucose intolerance by some clinical reports (Lee et al., 1999; Reynolds et al., 2001). Therefore, our findings suggest that inactivation of the Gadd45 β DNA methylation machinery may serve as a potential avenue for treating T2DM, including long-term GC exposure-associated diabetes.

Materials and methods

Animal studies

8-wk-old male *db/db* and *ob/ob* mice were purchased from the Nanjing Biomedical Research Institute of Nanjing University. 8–10-wk-old male C57BL/6J mice were purchased from the

Shanghai Laboratory Animal Company. HFD-induced obese mice were generated by feeding C57BL/6J mice an HFD (D12492; Research Diets) for 12 wk. The metabolic features of HFD, *ob/ob*, and *db/db* mice have been described in our previous study (Lu et al., 2014). Gadd45 β F/F mice obtained from GemPharmatech Co., Ltd. were generated by CRISPR/Cas9 technology (Fig. S4 A). Exons 1–4 of the Gadd45 β transcript are recommended as the KO region. Briefly, small guide RNA was transcribed in vitro, and a donor vector was constructed. Cas9, small guide RNA, and donor were microinjected into the fertilized eggs of C57BL/6J mice. Fertilized eggs were transplanted to obtain positive F0 mice, which were confirmed by PCR and sequencing. A stable F1 generation mouse model was obtained by mating positive F0 generation mice with C57BL/6J mice. To generate Gadd45 β LKO mice, 8-wk-old male Gadd45 β F/F mice were injected with AAV9-expressing Cre recombinase through the tail vein. The Gadd45 β F/F littermates injected with AAV9-expressing GFP recombinase were used as controls. All mice were housed at 21°C \pm 1°C with 55% \pm 10% humidity and a 12-h/12-h light/dark cycle. Dex (Sigma-Aldrich) or vehicle control was administered daily for 14 d at a dose of 1.0 mg/kg body weight by i.p. injection. Plasma insulin, glucagon, corticosterone, and β -hydroxybutyrate levels were measured using kits from Crystal Chem (90080), Crystal Chem (81518), Labor Diagnostika Nord (ARE-8100), and BioVision (K632), respectively. For analyzing hepatic TG content, liver tissues (~100 mg) were homogenized in 1 ml of 5% NP-40 solution and heated to 100°C and then cooled to room temperature. The tissue homogenates were centrifuged for 2 min, and the supernatants were processed to measure TG content using the Triglyceride Quantification Kit (K622; Bio-Vision). The animal protocol was reviewed and approved by the animal care committee of Shanghai Jiao Tong University School of Medicine.

Human studies

The human subjects were recruited from the fatty liver clinic of Zhongshan Hospital, Fudan University. Liver samples were collected from normal participants ($n = 13$, male) and patients with type 2 diabetes ($n = 16$, male) through ultrasonography-guided percutaneous needle liver biopsies. Subjects who had type 1 diabetes, chronic viral hepatitis, hypothyroidism, excessive use of alcohol, use of drugs that may affect glucose metabolism, abnormal renal function, or infectious diseases were excluded. Blood samples were collected after a 12-h overnight fast, and plasma was stored at -80°C for biochemical assays. The clinical characteristics of human subjects are shown in Table S4. The human study was approved by the human research ethics committee of Zhongshan Hospital, Fudan University. Written informed consent was obtained from each subject.

Ad infection

Briefly, full-length mouse Gadd45 β cDNA or the GFP gene was cloned into GV314 adenoviral vector (CMV-MCS-3FLAG-SV40-EGFP) from GeneChem. 2×10^9 PFU per mouse were delivered into C57BL/6 mice for 15 d. Ad-shRNA particles targeting GR, Gadd45 β , and PGC-1 α were generated using pAD_BLOCK_IT_DEST vectors (Invitrogen). The shRNAs had the following

sequences: GR (5'-AGAAATGACTGCCTTACTA-3'), Gadd45 β (5'-GCCACAATGACATTGACATCG-3'), PGC-1 α (5'-GGTGGATTG AAGTGGTGTAGA-3'), or TET1 (5'-GCCTCTTCTACGGGAACA TTC-3'). To knock down hepatic GR expression, 2×10^9 PFU per mouse were delivered into C57BL/6 or HFD mice for 7 d. To knock down hepatic Gadd45 β expression, 4×10^9 PFU per mouse were delivered into *db/db* mice for 14 d. All viruses were purified by the cesium chloride method, dialyzed in PBS containing 10% glycerol, and administered to mice through tail vein injection.

PTTs, GTTs, and ITTs

For the PTTs and GTTs, mice were fasted for 16 h and injected i.p. with pyruvate (1.5 g/kg body weight; Sigma-Aldrich) or D-glucose (1.5 g/kg body weight; Sigma-Aldrich). For the ITTs, mice were injected with regular human insulin (0.75 U/kg body weight; Eli Lilly) after a 6-h fast. Blood glucose was collected from tail veins after injection and measured by a portable blood glucose meter (Johnson & Johnson).

mRNA sequencing

High-throughput mRNA sequencing service was provided by CloudSeq Biotech. Total RNA (1 μg) was used for removing the ribosomal RNAs (rRNAs) using Ribo-Zero rRNA removal kits (Illumina) following the manufacturer's instructions. RNA libraries were constructed using rRNA-depleted RNAs with the TruSeq Stranded Total RNA Library Prep Kit (Illumina) according to the manufacturer's instructions. Libraries were controlled for quality and quantified using the BioAnalyzer 2100 system (Agilent Technologies, Inc.). Libraries were denatured as single-stranded DNA molecules, captured on Illumina flow cells, amplified in situ as clusters, and finally sequenced for 150 cycles on an Illumina HiSeq Sequencer according to the manufacturer's instructions. Paired-end reads were harvested from the Illumina HiSeq 4000 sequencer and were quality controlled by Q30. After 3' adaptor trimming and low-quality read removal by Cutadapt software (version 1.9.3), the high-quality clean reads were aligned to the reference genome (University of California, Santa Cruz [UCSC] Genome Browser hg19) with HISAT2 software (version 2.0.4). Then, guided by the Ensembl GTF gene annotation file, Cuffdiff software (part of cufflinks) was used to get the gene-level fragments per kilobase million as the expression profiles of mRNA. Fold change and P value were calculated based on fragments per kilobase million, and differentially expressed mRNAs were identified. The RNA-seq data have been deposited in the Gene Expression Omnibus database (GSE159038 and GSE159084).

Cell culture

HepG2 cells were obtained from the Cell Bank of Shanghai Institute of Biochemistry and Cell Biology (Chinese Academy of Sciences). MPHs were isolated from the livers of 10-wk-old male C57BL/6 mice by collagenase perfusion through the portal vein and purified by centrifugation. Freshly prepared MPHs were resuspended in attachment media (Science Cell) and seeded in 6-well plates at a final density of 5×10^5 cells per well. 12 h later, unattached cells were washed away, and DMEM (Gibco-BRL) was added for an overnight incubation.

Glucose production assays

MPHs were infected with Ads as indicated for 36 h. Then, the medium was replaced with glucose-free DMEM supplemented with 2 mM sodium pyruvate and 20 mM sodium lactate. 4 h later, media were collected, and the glucose concentrations were measured with a colorimetric glucose assay kit (MAK263; Sigma-Aldrich). The readings were normalized to total protein contents determined from the whole-cell extracts.

Plasmids construction and luciferase reporter assays

HA-tagged full-length mouse GR and Gadd45 β expression plasmids were cloned by PCR amplification and inserted into porcine cytomegalovirus vector with HindIII/BamHI restriction sites. The promoter region of the mouse Gadd45 β gene extending from position -2,000 bp (relative to the mRNA transcription start site) to +1 was cloned into the PGL4.12 luciferase reporter plasmid with the XhoI/HindIII restriction sites. Mutant GRE motif was generated using the QuikChange II XL Site-Directed Mutagenesis Kit (Agilent Technologies Inc.) with the following primers (mutation sites underlined): mutant 1: 5'-CATTCCAAG TGGGCTCTCCCCCTCCCTTTCCGGAAG-3'; mutant 2: 5'-AAG GCCCGGCAGGGCACTTAGTAAGCCTCCTGGCGCAT-3'. For luciferase assays, HepG2 cells were placed in 24-well plates and cotransfected with GR expression plasmids and luciferase reporter plasmids using Lipofectamine 3000 (Thermo Fisher Scientific) according to the manufacturer's instructions. The plasmid expressing Renilla luciferase with thymidine kinase promoter (Promega) was used to normalize the luciferase activity. 24 h after transfection, cells were treated with Dex (10 nM) or vehicle for 12 h before harvest. Luciferase activities were measured using the Dual-Luciferase Reporter Assay System (Promega).

ChIP

ChIP assays were performed using the EZ ChIP kit (Merck Millipore). MPHs or minced liver tissues were fixed in 1% formaldehyde (Sigma-Aldrich) for 10 min. Cross-linking was stopped by addition of glycine at a concentration of 125 mM for 5 min, followed by centrifugation and washing in SDS lysis buffer at room temperature. DNA was sheared to fragments of 200–1,000 bp by sonication. Lysates containing soluble chromatin were incubated and precipitated overnight with 5 μ g anti-GR antibody (ab3579; Abcam), anti-TET1 (ab191698; Abcam), anti-TET2 (ab94580; Cell Signaling Technology), anti-TET3 (ab139311; Abcam), or IgG (ab172730; Abcam). DNA-protein immune complexes were removed with protein G agarose and then washed and eluted. Protein-DNA cross-links were reversed by treatment with proteinase K for 2 h at 45°C. The DNA was subsequently purified, diluted, and subjected to qRT-PCR. The mouse Gadd45 β gene promoter fragments containing the GRE motif were amplified using the following primers: site 1: 5'-TCT CACTTTGGGGAGAGATC-3' (forward), 5'-GAGTCCCTAGCC TTTCCCA-3' (reverse); site 2: 5'-TTCGAGGCCAGCCTGGTCTA-3' (forward), 5'-CCTCATGAGGTCTCTGCTCA-3' (reverse). The promoter region of the GAPDH proximal promoter was set as the negative control. Primers for the GAPDH promoter were: 5'-CTA TCCTGGGAACCATCA-3' (forward) and 5'-AAGCGTGTGGGC TCCGAA-3' (reverse).

MeDIP-seq

Genomic DNA from mouse livers was isolated using phenol-chloroform, precipitated with ethanol, and sonicated to 100–500 bp using Bioruptor (Diagenode). Sonicated DNA was end repaired, A tailed, and ligated to adaptors by using the NEBNext Ultra DNA Library Prep Kit (New England Biolabs). Then, MeDIP was performed with an mAb against 5mC by following the standard manufacturer's protocol (MilliporeSigma). MeDIP DNA libraries were quantified using Quant-iT PicoGreen double-strand DNA kits (Life Technologies) and subjected to high-throughput 150-base paired end sequencing on an Illumina HiSeq sequencer according to the manufacturer's recommended protocol. High-quality reads (raw data) were generated after sequencing, image analysis, base calling, and quality filtering on an Illumina sequencer. Cutadapt software was used for adaptor trimming. After adaptor trimming, the trimmed reads were aligned to the mouse genome (UCSC Genome Browser, mm10) using BOWTIE software (version 2.1.0) with default parameters. Peak calling was performed by MACS1.4 software. DMRs were identified by DiffReps software. The enriched peaks and DMRs were then annotated with the UCSC RefSeq database to connect the peak information with the gene annotation. The enriched peaks were visualized on the UCSC Genome Browser.

MeDIP-PCR

Purified genomic DNA (4 μ g) was fragmented to a mean size of 300 bp using a Covaris machine, denatured, and immunoprecipitated with antibodies against 5mC (MilliporeSigma) or 5hmC (MilliporeSigma). Immunoprecipitated DNA was recovered with proteinase K digestion followed by column-based purification (DNA Wizard; Promega). Recovered DNA fractions were diluted 1:50 and measured using RT-PCR with an ABI PRISM 7000 sequence detector system and fluorescence-based SYBR Green technology (Applied Biosystems).

Pyrosequencing

DNA methylation levels were determined by pyrosequencing after bisulfite conversion using the EpiTect bisulfite kit (Qiagen; Wu et al., 2016). Quantitative PCR was performed on a PSQ 96MD system with the PyroGold sequence analysis reagent kit (Qiagen), and results were analyzed using the PyroMark CpG software (version 1.0.11.14; Qiagen). The quantitative accuracy and sensitivity of our pyrosequencing assays have been validated using mixtures of fully methylated and unmethylated mouse genomic DNA at different ratios (A&D Technology Corporation).

RNA isolation and qRT-PCR

Total RNAs from mouse livers or MPHs were extracted using TRIzol reagent (Invitrogen). RNA purity and concentrations were measured using the NanoDrop ONE spectrophotometer (Thermo Fisher Scientific). The mRNAs were reverse transcribed into cDNA using the Promega Reverse Transcription System. Oligo(dT) was used to prime cDNA synthesis. cDNA was stored at -20°C before use. qRT-PCR was performed using SYBR Green Premix Ex Taq (Takara Bio) on a Light Cycler 480 (Roche),

and data were analyzed by the comparative cycle threshold method. PCR conditions included an initial holding period at 95°C for 5 min, followed by a two-step PCR program consisting of 95°C for 5 s and 60°C for 30 s for 50 cycles. Relative abundance of mRNA was normalized to ribosomal protein 36B4. The primer sequences are available upon request.

Western blots

To prepare total protein extracts, liver tissues and primary hepatocytes were lysed in RIPA buffer containing 50 mM Tris-HCl, 150 mM NaCl, 5 mM MgCl₂, 2 mM EDTA, 1 mM NaF, 1% NP-40, and 0.1% SDS. Equivalent amounts of protein samples were denatured in loading buffer and resolved by 10–12% SDS-PAGE and transferred onto polyvinylidene fluoride membranes. Membranes were blocked in 5% nonfat milk for 1 h before incubation with primary antibody overnight at 4°C. Membranes were washed with PBS with Tween-20 five times and incubated with secondary antibody for 1 h. The signals of the proteins were then visualized by an electrochemiluminescence system. The following primary antibodies were used: anti-Gadd45β at 1:2,000 (sc-377311; Santa Cruz Biotechnology), anti-PGC-1α at 1:2,000 (AB3242; EMD Millipore), anti-TET1 at 1:1,000 (61741; Active Motif), anti-TRB3 at 1:1,000 (sc-365842; Santa Cruz Biotechnology), anti-p-AKT at 1:1,000 (4060; Cell Signaling Technology), anti-t-AKT at 1:2,000 (9272; Cell Signaling Technology), and anti-GAPDH antibody at 1:6,000 (KC-5G5; Kangchen Technology).

Statistics

Data are presented as mean ± SEM. For animal and cellular experiments, a two-tailed unpaired Student's *t* test was performed to compare two groups. One-way ANOVA followed by the Student-Newman-Keuls test was used to compare more than two groups. The correlation between mRNA expression levels of target genes and plasma glucose levels was analyzed by Pearson correlation. *P* values <0.05 were considered statistically significant. *, **, and *** represent *P* < 0.05, *P* < 0.01, and *P* < 0.001, respectively.

Online supplemental material

Fig. S1 shows the up-regulation of hepatic Gadd45β by GCs. Fig. S2 shows the identification of PGC-1α as a target of Gadd45β. Fig. S3 shows the methylation status of gluconeogenic genes. Fig. S4 shows the generation of Gadd45β LKO mice and the methylation status and expression of hepatic gluconeogenic genes in diabetes. Fig. S5 shows the hepatic insulin signaling and lipid metabolism in mice. Table S1 shows the up-regulated genes by RNA-seq analysis. Table S2 shows the overlap of the up-regulated expressed genes. Table S3 shows the overlap of the down-regulated expressed genes. Table S4 shows the clinical characteristics of human subjects.

Acknowledgments

We thank Professor Peng Li (Institute of Metabolism and Integrative Biology, Fudan University, Shanghai, China) and Professor Guoliang Xu (Shanghai Institute of Biochemistry and Cell Biology, Shanghai, China) for critical discussion of the data.

This work is supported by the National Natural Science Foundation of China (81722013 to Y. Lu, 81771574 to L. Wu, 81900727 to Y. Jiao, 82070887 to Y. Li), the National Key Research and Development Program of China (2018YFA0800402 to Y. Lu), the Shanghai Municipal Commission of Health and Family Planning Foundation (20174Y0036 to L. Wu), the Shanghai Sailing Program (19YF1406900 to Y. Jiao), and the Shanghai Science Foundation (18ZR1437800 to Y. Li).

Author contributions: Y. Lu designed and directed experiments; L. Wu, Y. Jiao, and Y. Li performed animal and cellular experiments; M. Li, B. Li, and Z. Yan contributed to animal and cellular experiments; J. Jiang and L. Zhao performed human experiments; X. Chen and X. Li contributed to overall experimental analysis and discussion. L. Wu, Y. Jiao, and Y. Lu wrote the manuscript. Y. Lu supervised the entire project and edited the manuscript. All authors reviewed the manuscript and provided final approval for submission.

Disclosures: The authors declare no competing interests exist.

Submitted: 19 July 2020

Revised: 5 August 2020

Accepted: 14 January 2021

References

- Ahrens, M., O. Ammerpohl, W. von Schönfels, J. Kolarova, S. Bens, T. Itzel, A. Teufel, A. Herrmann, M. Brosch, H. Hinrichsen, et al. 2013. DNA methylation analysis in nonalcoholic fatty liver disease suggests distinct disease-specific and remodeling signatures after bariatric surgery. *Cell Metab.* 18:296–302. <https://doi.org/10.1016/j.cmet.2013.07.004>
- Barrès, R., M.E. Osler, J. Yan, A. Rune, T. Fritz, K. Caidahl, A. Krook, and J.R. Zierath. 2009. Non-CpG methylation of the PGC-1α promoter through DNMT3B controls mitochondrial density. *Cell Metab.* 10: 189–198. <https://doi.org/10.1016/j.cmet.2009.07.011>
- Barrès, R., J. Yan, B. Egan, J.T. Treebak, M. Rasmussen, T. Fritz, K. Caidahl, A. Krook, D.J. O'Gorman, and J.R. Zierath. 2012. Acute exercise remodels promoter methylation in human skeletal muscle. *Cell Metab.* 15:405–411. <https://doi.org/10.1016/j.cmet.2012.01.001>
- Bayraktar, G., and M.R. Kreutz. 2018. The role of activity-dependent DNA demethylation in the adult brain and in neurological disorders. *Front. Mol. Neurosci.* 11:169. <https://doi.org/10.3389/fnmol.2018.00169>
- Bhalla, K., W.J. Liu, K. Thompson, L. Anders, S. Devarakonda, R. Dewi, S. Buckley, B.J. Hwang, B. Polster, S.G. Dorsey, et al. 2014. Cyclin D1 represses gluconeogenesis via inhibition of the transcriptional coactivator PGC1α. *Diabetes.* 63:3266–3278. <https://doi.org/10.2337/db13-1283>
- Chadwick, J.A., J.S. Hauck, J. Lowe, J.J. Shaw, D.C. Guttridge, C.E. Gomez-Sanchez, E.P. Gomez-Sanchez, and J.A. Rafael-Fortney. 2015. Mineralocorticoid receptors are present in skeletal muscle and represent a potential therapeutic target. *FASEB J.* 29:4544–4554. <https://doi.org/10.1096/fj.15-276782>
- Chen, X., N. Iqbal, and G. Boden. 1999. The effects of free fatty acids on gluconeogenesis and glycogenolysis in normal subjects. *J. Clin. Invest.* 103:365–372. <https://doi.org/10.1172/JCI5479>
- Dassonville, J., F. Díaz-Castro, C. Donoso-Barraza, C. Sepúlveda, F. Pino-de la Fuente, P. Pino, A. Espinosa, M. Chiong, M. Llanos, and R. Troncoso. 2020. Moderate aerobic exercise training prevents the augmented hepatic glucocorticoid response induced by high-fat diet in mice. *Int. J. Mol. Sci.* 21:7582. <https://doi.org/10.3390/ijms21207582>
- Fuhrmeister, J., A. Zota, T.P. Sijmonsma, O. Seibert, S. Cingir, K. Schmidt, N. Vallon, R.M. de Guia, K. Niopek, M. Berriel Diaz, et al. 2016. Fasting-induced liver GADD45β restrains hepatic fatty acid uptake and improves metabolic health. *EMBO Mol. Med.* 8:654–669. <https://doi.org/10.15252/emmm.201505801>
- Goldstein, I., and G.L. Hager. 2015. Transcriptional and chromatin regulation during fasting – the genomic era. *Trends Endocrinol. Metab.* 26:699–710. <https://doi.org/10.1016/j.tem.2015.09.005>

- Herzig, S., F. Long, U.S. Jhala, S. Hedrick, R. Quinn, A. Bauer, D. Rudolph, G. Schutz, C. Yoon, P. Puigserver, et al. 2001. CREB regulates hepatic gluconeogenesis through the coactivator PGC-1. *Nature*. 413:179-183. <https://doi.org/10.1038/35093131>
- Jarukamjorn, K., T. Sakuma, M. Yamamoto, A. Ohara, and N. Nemoto. 2001. Sex-associated expression of mouse hepatic and renal CYP2B enzymes by glucocorticoid hormones. *Biochem. Pharmacol.* 62:161-169. [https://doi.org/10.1016/S0006-2952\(01\)00656-6](https://doi.org/10.1016/S0006-2952(01)00656-6)
- Kersten, S., J. Seydoux, J.M. Peters, F.J. Gonzalez, B. Desvergne, and W. Wahli. 1999. Peroxisome proliferator-activated receptor alpha mediates the adaptive response to fasting. *J. Clin. Invest.* 103:1489-1498. <https://doi.org/10.1172/JCI6223>
- Koo, S.H., H. Satoh, S. Herzig, C.H. Lee, S. Hedrick, R. Kulkarni, R.M. Evans, J. Olefsky, and M. Montminy. 2004. PGC-1 promotes insulin resistance in liver through PPAR-alpha-dependent induction of TRB-3. *Nat. Med.* 10: 530-534. <https://doi.org/10.1038/nm1044>
- Laker, R.C., T.S. Lillard, M. Okutsu, M. Zhang, K.L. Hoehn, J.J. Connelly, and Z. Yan. 2014. Exercise prevents maternal high-fat diet-induced hypermethylation of the Pgc-1a gene and age-dependent metabolic dysfunction in the offspring. *Diabetes*. 63:1605-1611. <https://doi.org/10.2337/db13-1614>
- Larsen, C.M., M.G. Døssing, S. Papa, G. Franzoso, N. Billestrup, and T. Mandrup-Poulsen. 2006. Growth arrest- and DNA-damage-inducible 45beta gene inhibits c-Jun N-terminal kinase and extracellular signal-regulated kinase and decreases IL-1beta-induced apoptosis in insulin-producing INS-1E cells. *Diabetologia*. 49:980-989. <https://doi.org/10.1007/s00125-006-0164-0>
- Lee, Z.S., J.C. Chan, V.T. Yeung, C.C. Chow, M.S. Lau, G.T. Ko, J.K. Li, C.S. Cockram, and J.A. Critchley. 1999. Plasma insulin, growth hormone, cortisol, and central obesity among young Chinese type 2 diabetic patients. *Diabetes Care*. 22:1450-1457. <https://doi.org/10.2337/diacare.22.9.1450>
- Lee, Y., J.E. Dominy, Y.J. Choi, M. Jurczak, N. Tolliday, J.P. Camporez, H. Chim, J.H. Lim, H.B. Ruan, X. Yang, et al. 2014. Cyclin D1-Cdk4 controls glucose metabolism independently of cell cycle progression. *Nature*. 510:547-551. <https://doi.org/10.1038/nature13267>
- Leone, T.C., J.J. Lehman, B.N. Finck, P.J. Schaeffer, A.R. Wende, S. Boudina, M. Courtois, D.F. Wozniak, N. Sambandam, C. Bernal-Mizrachi, et al. 2005. PGC-1alpha deficiency causes multi-system energy metabolic derangements: muscle dysfunction, abnormal weight control and hepatic steatosis. *PLoS Biol.* 3:e101. <https://doi.org/10.1371/journal.pbio.0030101>
- Li, Z., T.P. Gu, A.R. Weber, J.Z. Shen, B.Z. Li, Z.G. Xie, R. Yin, F. Guo, X. Liu, F. Tang, et al. 2015. Gadd45a promotes DNA demethylation through TDG. *Nucleic Acids Res.* 43:3986-3997. <https://doi.org/10.1093/nar/gkv283>
- Liang, Q., L. Zhong, J. Zhang, Y. Wang, S.R. Bornstein, C.R. Triggle, H. Ding, K.S. Lam, and A. Xu. 2014. FGF21 maintains glucose homeostasis by mediating the cross talk between liver and brain during prolonged fasting. *Diabetes*. 63:4064-4075. <https://doi.org/10.2337/db14-0541>
- Lin, J., P.H. Wu, P.T. Tarr, K.S. Lindenberg, J. St-Pierre, C.Y. Zhang, V.K. Mootha, S. Jäger, C.R. Vianna, R.M. Reznick, et al. 2004. Defects in adaptive energy metabolism with CNS-linked hyperactivity in PGC-1alpha null mice. *Cell*. 119:121-135. <https://doi.org/10.1016/j.cell.2004.09.013>
- Lin, J., C. Handschin, and B.M. Spiegelman. 2005. Metabolic control through the PGC-1 family of transcription coactivators. *Cell Metab.* 1:361-370. <https://doi.org/10.1016/j.cmet.2005.05.004>
- Ling, C., and T. Rönn. 2019. Epigenetics in human obesity and type 2 diabetes. *Cell Metab.* 29:1028-1044. <https://doi.org/10.1016/j.cmet.2019.03.009>
- Liu, Y., Y. Nakagawa, Y. Wang, R. Li, X. Li, T. Ohzeki, and T.C. Friedman. 2003. Leptin activation of corticosterone production in hepatocytes may contribute to the reversal of obesity and hyperglycemia in leptin-deficient ob/ob mice. *Diabetes*. 52:1409-1416. <https://doi.org/10.2337/diabetes.52.6.1409>
- Liu, Y., Y. Nakagawa, Y. Wang, R. Sakurai, P.V. Tripathi, K. Lutfy, and T.C. Friedman. 2005. Increased glucocorticoid receptor and 11beta-hydroxysteroid dehydrogenase type 1 expression in hepatocytes may contribute to the phenotype of type 2 diabetes in db/db mice. *Diabetes*. 54:32-40. <https://doi.org/10.2337/diabetes.54.1.32>
- Liu, Y., C. Yan, Y. Wang, Y. Nakagawa, N. Nerio, A. Anghel, K. Lutfy, and T.C. Friedman. 2006. Liver X receptor agonist T0901317 inhibition of glucocorticoid receptor expression in hepatocytes may contribute to the amelioration of diabetic syndrome in db/db mice. *Endocrinology*. 147: 5061-5068. <https://doi.org/10.1210/en.2006-0243>
- Liu, J., D. Ibi, K. Taniguchi, J. Lee, H. Herrema, B. Akosman, P. Mucka, M.A. Salazar Hernandez, M.F. Uyar, S.W. Park, et al. 2016. Inflammation improves glucose homeostasis through IKKβ-XBPs interaction. *Cell*. 167:1052-1066.e18. <https://doi.org/10.1016/j.cell.2016.10.015>
- Lu, Y., Z. Zhang, X. Xiong, X. Wang, J. Li, G. Shi, J. Yang, X. Zhang, H. Zhang, J. Hong, et al. 2012. Glucocorticoids promote hepatic cholestasis in mice by inhibiting the transcriptional activity of the farnesoid X receptor. *Gastroenterology*. 143:1630-1640.e8. <https://doi.org/10.1053/j.gastro.2012.08.029>
- Lu, Y., X. Liu, Y. Jiao, X. Xiong, E. Wang, X. Wang, Z. Zhang, H. Zhang, L. Pan, Y. Guan, et al. 2014. Perioestin promotes liver steatosis and hypertriglyceridemia through downregulation of PPARα. *J. Clin. Invest.* 124: 3501-3513. <https://doi.org/10.1172/JCI74438>
- Lu, Y., E. Wang, Y. Chen, B. Zhou, J. Zhao, L. Xiang, Y. Qian, J. Jiang, L. Zhao, X. Xiong, et al. 2020. Obesity-induced excess of 17-hydroxyprogesterone promotes hyperglycemia through activation of glucocorticoid receptor. *J. Clin. Invest.* 130:3791-3804. <https://doi.org/10.1172/JCI134485>
- Ma, D.K., M.H. Jang, J.U. Guo, Y. Kitabatake, M.L. Chang, N. Pow-Anpongkul, R.A. Flavell, B. Lu, G.L. Ming, and H. Song. 2009. Neuronal activity-induced Gadd45b promotes epigenetic DNA demethylation and adult neurogenesis. *Science*. 323:1074-1077. <https://doi.org/10.1126/science.1166859>
- Martinez, D., T. Pentinat, S. Ribó, C. Daviaud, V.W. Bloks, J. Cebrià, N. Vilalmanzo, S.G. Kalko, M. Ramón-Krauel, R. Díaz, et al. 2014. In utero undernutrition in male mice programs liver lipid metabolism in the second-generation offspring involving altered LXRα DNA methylation. *Cell Metab.* 19:941-951. <https://doi.org/10.1016/j.cmet.2014.03.026>
- Messeguer, X., R. Escudero, D. Farré, O. Núñez, J. Martínez, and M.M. Albà. 2002. PROMO: detection of known transcription regulatory elements using species-tailored searches. *Bioinformatics*. 18:333-334. <https://doi.org/10.1093/bioinformatics/18.2.333>
- Mouchiroud, L., L.J. Eichner, R.J. Shaw, and J. Auwerx. 2014. Transcriptional coregulators: fine-tuning metabolism. *Cell Metab.* 20:26-40. <https://doi.org/10.1016/j.cmet.2014.03.027>
- Okamoto, H., E. Latres, R. Liu, K. Thabet, A. Murphy, D. Valenzeula, G.D. Yancopoulos, T.N. Stitt, D.J. Glass, and M.W. Sleeman. 2007. Genetic deletion of Trb3, the mammalian *Drosophila tribbles* homolog, displays normal hepatic insulin signaling and glucose homeostasis. *Diabetes*. 56: 1350-1356. <https://doi.org/10.2337/db06-1448>
- Owen, H.C., S.J. Roberts, S.F. Ahmed, and C. Farquharson. 2008. Dexamethasone-induced expression of the glucocorticoid response gene lipocalin 2 in chondrocytes. *Am. J. Physiol. Endocrinol. Metab.* 294: E1023-E1034. <https://doi.org/10.1152/ajpendo.00586.2007>
- Petersen, M.C., D.F. Vatner, and G.I. Shulman. 2017. Regulation of hepatic glucose metabolism in health and disease. *Nat. Rev. Endocrinol.* 13: 572-587. <https://doi.org/10.1038/nrendo.2017.80>
- Piccini, E., G. Villani, and A. Moschetta. 2019. Metabolic aspects in NAFLD, NASH and hepatocellular carcinoma: the role of PGC1 coactivators. *Nat. Rev. Gastroenterol. Hepatol.* 16:160-174. <https://doi.org/10.1038/s41575-018-0089-3>
- Quagliarini, F., A.A. Mir, K. Balazs, M. Wierer, K.A. Dyar, C. Jouffe, K. Makris, J. Hawe, M. Heinig, F.V. Philipp, et al. 2019. Cistronic reprogramming of the diurnal glucocorticoid hormone response by high-fat diet. *Mol. Cell*. 76:531-545.e5. <https://doi.org/10.1016/j.molcel.2019.10.007>
- Reynolds, R.M., B.R. Walker, H.E. Syddall, C.B. Whorwood, P.J. Wood, and D.I. Phillips. 2001. Elevated plasma cortisol in glucose-intolerant men: differences in responses to glucose and habituation to venepuncture. *J. Clin. Endocrinol. Metab.* 86:1149-1153. <https://doi.org/10.1210/jcem.86.3.7300>
- Rines, A.K., K. Sharabi, C.D. Tavares, and P. Puigserver. 2016. Targeting hepatic glucose metabolism in the treatment of type 2 diabetes. *Nat. Rev. Drug Discov.* 15:786-804. <https://doi.org/10.1038/nrd.2016.151>
- Roden, M., H. Stingl, V. Chandramouli, W.C. Schumann, A. Hofer, B.R. Landau, P. Nowotny, W. Waldhäusl, and G.I. Shulman. 2000. Effects of free fatty acid elevation on postabsorptive endogenous glucose production and gluconeogenesis in humans. *Diabetes*. 49:701-707. <https://doi.org/10.2337/diabetes.49.5.701>
- Roqueta-Rivera, M., R.M. Esquejo, P.E. Phelan, K. Sandor, B. Daniel, F. Foulfelle, J. Ding, X. Li, S. Khorasanizadeh, and T.F. Osborne. 2016. SETDB2 links glucocorticoid to lipid metabolism through Insig2a regulation. *Cell Metab.* 24:474-484. <https://doi.org/10.1016/j.cmet.2016.07.025>
- Rose, A.J., and S. Herzig. 2013. Metabolic control through glucocorticoid hormones: an update. *Mol. Cell. Endocrinol.* 380:65-78. <https://doi.org/10.1016/j.mce.2013.03.007>
- Schäfer, A. 2013. Gadd45 proteins: key players of repair-mediated DNA demethylation. *Adv. Exp. Med. Biol.* 793:35-50. https://doi.org/10.1007/978-1-4614-8289-5_3

- Schüle, K.M., M. Leichsenring, T. Andreani, V. Vastolo, M. Mallick, M.U. Musheev, E. Karaulanov, and C. Niehrs. 2019. GADD45 promotes locus-specific DNA demethylation and 2C cycling in embryonic stem cells. *Genes Dev.* 33:782–798. <https://doi.org/10.1101/gad.325696.119>
- Sharabi, K., H. Lin, C.D.J. Tavares, J.E. Dominy, J.P. Camporez, R.J. Perry, R. Schilling, A.K. Rines, J. Lee, M. Hickey, et al. 2017. Selective chemical inhibition of PGC-1 α gluconeogenic activity ameliorates type 2 diabetes. *Cell.* 169:148–160.e15. <https://doi.org/10.1016/j.cell.2017.03.001>
- Solomon, S.S., O. Odunusi, D. Carrigan, G. Majumdar, D. Kakoola, N.I. Lenchik, and I.C. Gerling. 2010. TNF- α inhibits insulin action in liver and adipose tissue: a model of metabolic syndrome. *Horm. Metab. Res.* 42:115–121. <https://doi.org/10.1055/s-0029-1241834>
- Staeher, P., O. Hother-Nielsen, B.R. Landau, V. Chandramouli, J.J. Holst, and H. Beck-Nielsen. 2003. Effects of free fatty acids per se on glucose production, gluconeogenesis, and glycogenolysis. *Diabetes.* 52:260–267. <https://doi.org/10.2337/diabetes.52.2.260>
- Sun, Z., and M.A. Lazar. 2013. Dissociating fatty liver and diabetes. *Trends Endocrinol. Metab.* 24:4–12. <https://doi.org/10.1016/j.tem.2012.09.005>
- Sunny, N.E., E.J. Parks, J.D. Browning, and S.C. Burgess. 2011. Excessive hepatic mitochondrial TCA cycle and gluconeogenesis in humans with nonalcoholic fatty liver disease. *Cell Metab.* 14:804–810. <https://doi.org/10.1016/j.cmet.2011.11.004>
- Wahl, S., A. Drong, B. Lehne, M. Loh, W.R. Scott, S. Kunze, P.C. Tsai, J.S. Ried, W. Zhang, Y. Yang, et al. 2017. Epigenome-wide association study of body mass index, and the adverse outcomes of adiposity. *Nature.* 541: 81–86. <https://doi.org/10.1038/nature20784>
- Wray, J.R., A. Davies, C. Sefton, T.J. Allen, A. Adamson, P. Chapman, B.Y.H. Lam, G.S.H. Yeo, A.P. Coll, E. Harno, et al. 2019. Global transcriptomic analysis of the arcuate nucleus following chronic glucocorticoid treatment. *Mol. Metab.* 26:5–17. <https://doi.org/10.1016/j.molmet.2019.05.008>
- Wu, X., and Y. Zhang. 2017. TET-mediated active DNA demethylation: mechanism, function and beyond. *Nat. Rev. Genet.* 18:517–534. <https://doi.org/10.1038/nrg.2017.33>
- Wu, L., Y. Lu, Y. Jiao, B. Liu, S. Li, Y. Li, F. Xing, D. Chen, X. Liu, J. Zhao, et al. 2016. Paternal psychological stress reprograms hepatic gluconeogenesis in offspring. *Cell Metab.* 23:735–743. <https://doi.org/10.1016/j.cmet.2016.01.014>
- Yang, X., M. Downes, R.T. Yu, A.L. Bookout, W. He, M. Straume, D.J. Mangelsdorf, and R.M. Evans. 2006. Nuclear receptor expression links the circadian clock to metabolism. *Cell.* 126:801–810. <https://doi.org/10.1016/j.cell.2006.06.050>
- Yazdanyar, A., W. Quan, W. Jin, and X.C. Jiang. 2013. Liver-specific phospholipid transfer protein deficiency reduces high-density lipoprotein and non-high-density lipoprotein production in mice. *Arterioscler. Thromb. Vasc. Biol.* 33:2058–2064. <https://doi.org/10.1161/ATVBAHA.113.301628>
- Yoon, J.C., P. Puigserver, G. Chen, J. Donovan, Z. Wu, J. Rhee, G. Adelmant, J. Stafford, C.R. Kahn, D.K. Granner, et al. 2001. Control of hepatic gluconeogenesis through the transcriptional coactivator PGC-1. *Nature.* 413:131–138. <https://doi.org/10.1038/35093050>
- Yu, J., F. Xiao, Y. Guo, J. Deng, B. Liu, Q. Zhang, K. Li, C. Wang, S. Chen, and F. Guo. 2015. Hepatic phosphoserine aminotransferase 1 regulates insulin sensitivity in mice via tribbles homolog 3. *Diabetes.* 64:1591–1602. <https://doi.org/10.2337/db14-1368>
- Zhang, R.P., J.Z. Shao, and L.X. Xiang. 2011. GADD45A protein plays an essential role in active DNA demethylation during terminal osteogenic differentiation of adipose-derived mesenchymal stem cells. *J. Biol. Chem.* 286:41083–41094. <https://doi.org/10.1074/jbc.M111.258715>

Supplemental material

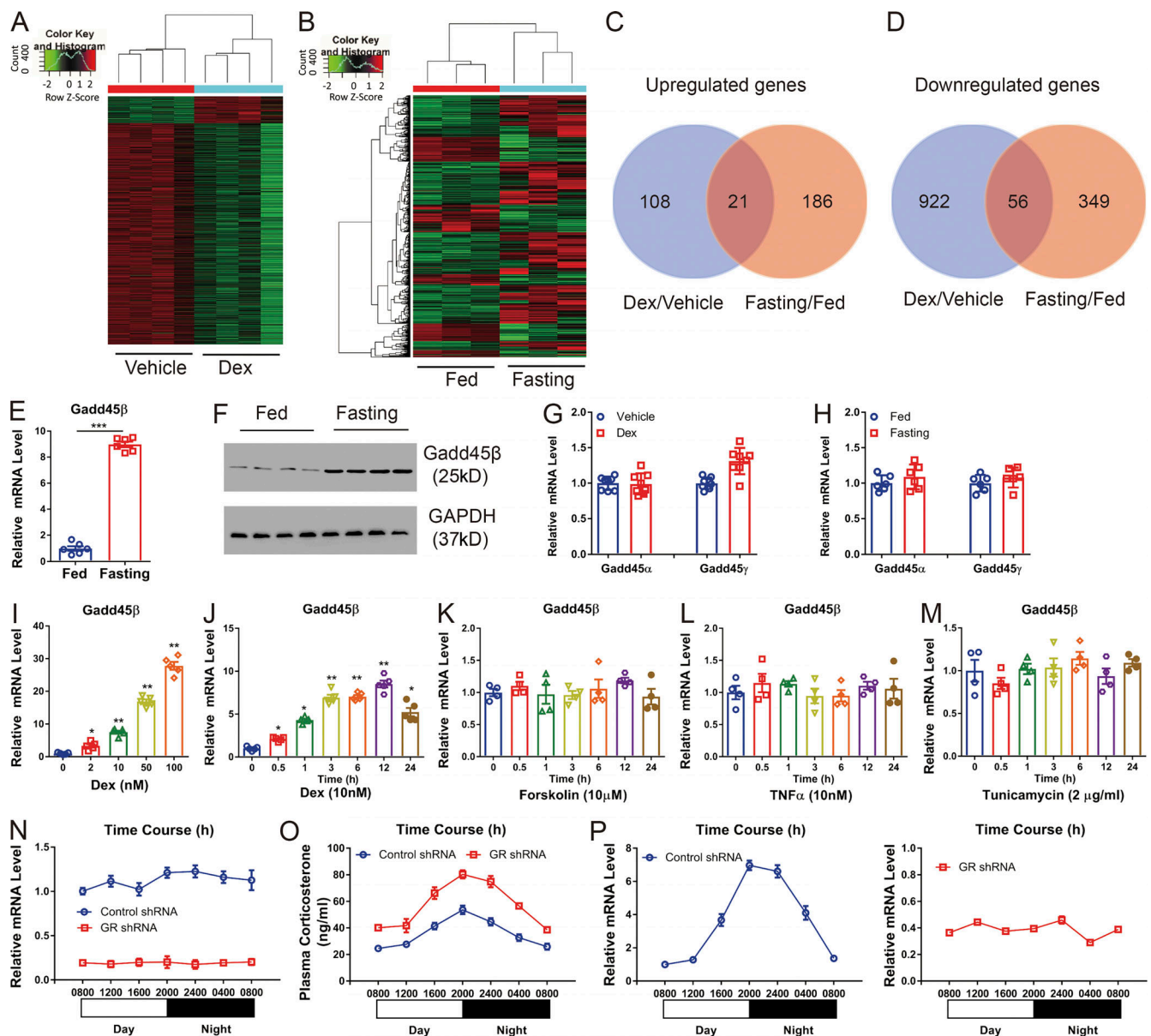


Figure S1. **Up-regulation of hepatic Gadd45β by glucocorticoids.** (A) Heatmap showing the fold change in mRNA levels in Dex-treated mouse livers relative to vehicle control. $n = 4$ per group. (B) Heatmap showing the fold change in mRNA levels in fasted mouse livers relative to fed conditions. $n = 3$ per group. (C) Overlap of the up-regulated expressed genes from Dex/vehicle control and fasting/fed livers. (D) Overlap of the down-regulated expressed genes from Dex/vehicle control and fasting/fed livers. (E) Relative mRNA levels of Gadd45β in the livers of C57BL/6 mice under ad libitum-fed or 16-h fasting conditions. $n = 5$ per group. (F) Protein levels of hepatic Gadd45β in two groups of mice as described in E. (G) Relative mRNA levels of Gadd45α and Gadd45γ in the livers of C57BL/6 mice treated with Dex (1.0 mg/kg) or vehicle control for 14 d. $n = 8$ per group. (H) Relative mRNA levels of Gadd45α and Gadd45γ in the livers of C57BL/6 mice under ad libitum feeding or 16-h fasting conditions. $n = 5$ per group. (I) Relative mRNA levels of Gadd45β in MPHs treated with different doses of Dex for 12 h. $n = 5$ per group. (J) Relative mRNA levels of Gadd45β in MPHs treated with Dex (10 nM) for different periods of time. $n = 5$ per group. (K–M) Relative mRNA levels of Gadd45β in MPHs treated with forskolin (K), TNFα (L), or tunicamycin (M) for different periods of time. $n = 4$ per group. (N–P) C57BL/6 mice were transfected with control adenoviral shRNA or GR-specific adenoviral shRNA for 7 d. $n = 5$ per group. (N) Relative mRNA levels of hepatic GR at the indicated time points in two groups of mice. (O) Circadian alteration of plasma corticosterone levels. (P) Relative mRNA levels of hepatic Gadd45β in two groups of mice. *, $P < 0.05$; **, $P < 0.01$; ***, $P < 0.001$. Two-tailed Student's t test (E, G, and H); one-way ANOVA (I–P). Data are combined from five (I and J) or four (K–M) independent experiments.

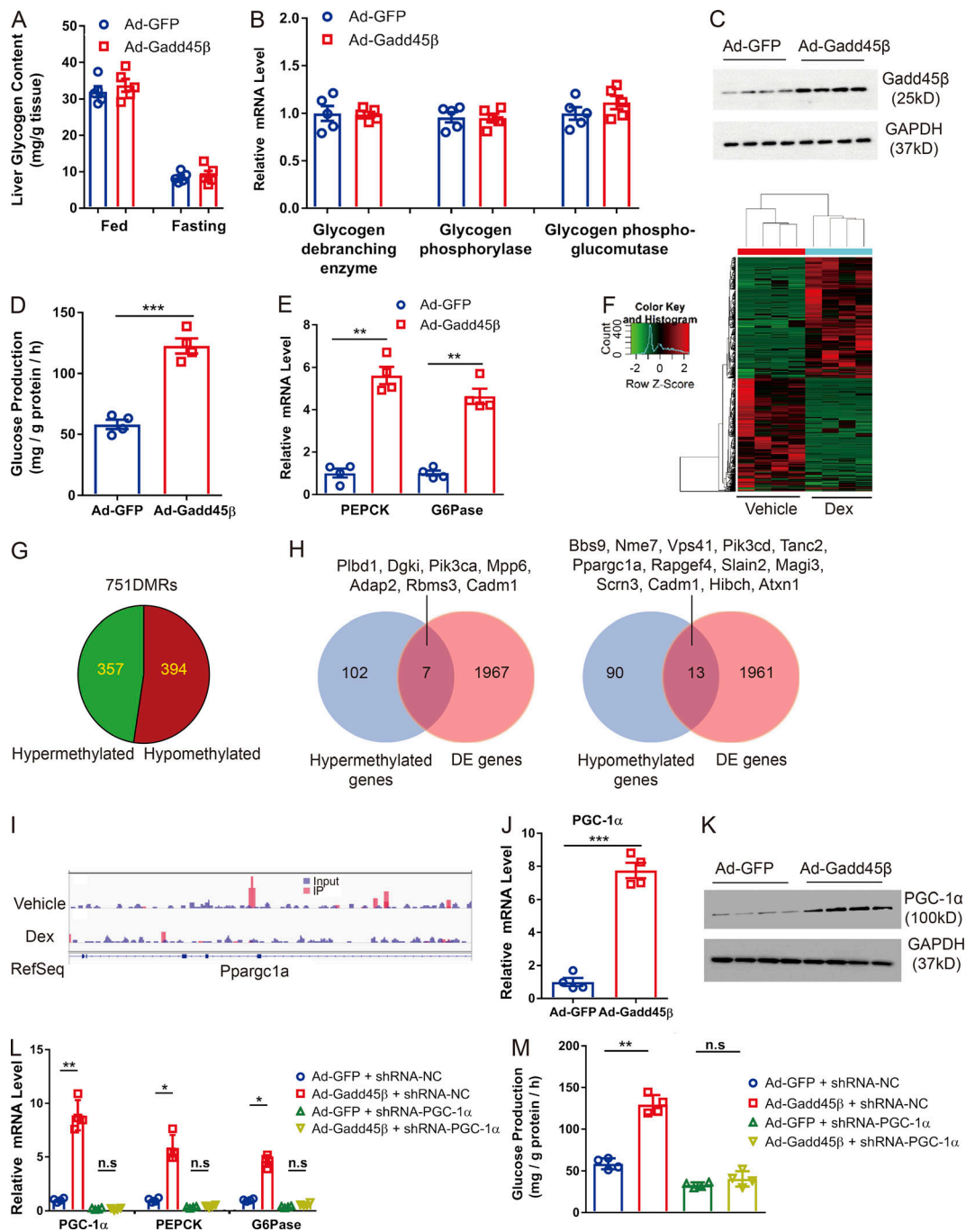


Figure S2. **Identification of PGC-1 α as a target of Gadd45 β .** (A and B) C57BL/6 mice were infected with Ad-GFP or Ad-Gadd45 β for 7 d. $n = 5$ per group. (A) Liver glycogen contents were measured in the livers of mice under fed or 16-h fasting conditions. (B) Relative mRNA levels of glycogenolysis-related genes in the livers of mice under 16-h fasting conditions. (C) Gadd45 β protein levels in MPHs infected with Ad-GFP or Ad-Gadd45 β for 24 h. (D) Glucose production in MPHs transfected with Ad-GFP or Ad-Gadd45 β . $n = 4$ per group. (E) Relative mRNA levels of PEPCK and G6Pase in MPHs transfected with Ad-GFP or Ad-Gadd45 β for 24 h. $n = 4$ per group. (F) A heatmap of the differentially methylated loci shows distinct patterns separating datasets obtained from the livers of mice treated with Dex or vehicle control. $n = 4$ per group. (G) Pie chart depicting the 751 DMRs showing differential methylation between Dex- and vehicle control-treated liver samples. (H) Overlap of hyper- (left) and hypomethylated (right) DMRs with differentially expressed (DE) genes. (I) Visualization of DNA methylation differences at the Ppargc1a gene. (J) Relative mRNA levels of PGC-1 α in MPHs transfected with Ad-GFP or Ad-Gadd45 β for 24 h. $n = 4$ per group. (K) PGC-1 α protein levels in MPHs infected with Ad-GFP or Ad-Gadd45 β . (L) Relative mRNA levels of PGC-1 α , PEPCK, and G6Pase in MPHs. Cells were infected with Ads as follows: Ad-GFP plus control shRNA (shRNA-NC), Ad-Gadd45 β plus shRNA-NC, Ad-GFP plus PGC-1 α shRNA (shRNA-PGC-1 α), Ad-Gadd45 β plus shRNA-PGC-1 α . $n = 4$ per group. (M) Glucose production in the MPHs described in L. $n = 4$ per group. Data are represented as mean \pm SEM. *, $P < 0.05$; **, $P < 0.01$; ***, $P < 0.001$. Two-tailed Student's t test (A, B, D, E, and J); one-way ANOVA (L and M). Data are combined from four (C–E and J–M) independent experiments. IP, immunoprecipitation.

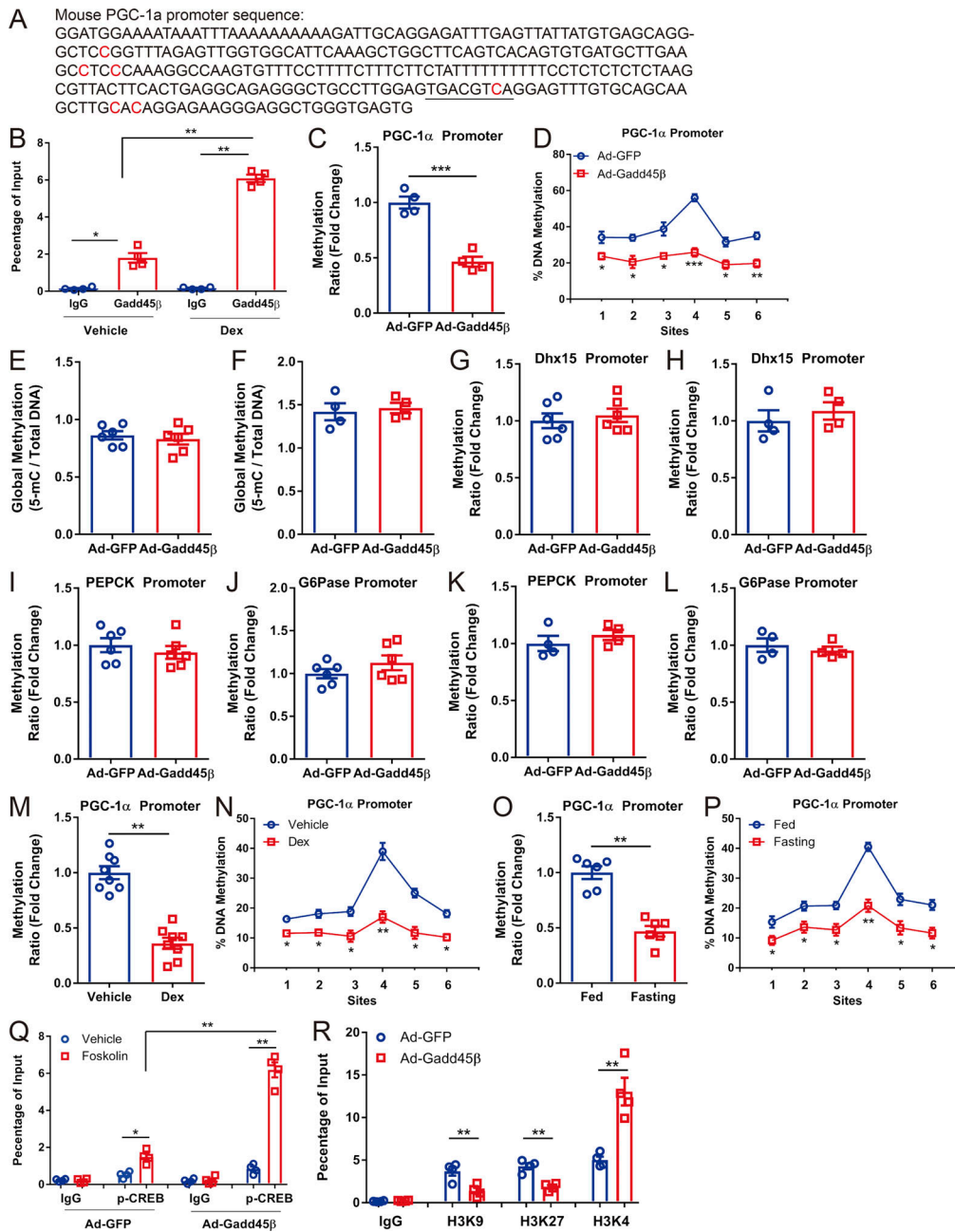


Figure S3. The methylation status of gluconeogenic genes. (A) The methylation sequencing region in the mouse PGC-1 α promoter. Methylated cytosines (C) are highlighted in red. The CREB binding site (5'-TGACGTCA-3') is underlined. (B) ChIP-qPCR assays showing the occupancy of Gadd45 β at the PGC-1 α promoter in the MPHs treated with vehicle control or Dex. $n = 4$ per group. (C) Promoter-specific methylation levels were analyzed by MeDIP-qPCR. The ratio of methylated DNA levels in Ad-GFP- or Ad-Gadd45 β -infected MPHs is presented. $n = 4$ per group. (D) The percentage of DNA methylation in individual methylated cytosine sites in Ad-GFP- or Ad-Gadd45 β -infected MPHs was analyzed by pyrosequencing. $n = 4$ per group. (E) Global DNA methylation ratio in livers from Ad-GFP- or Ad-Gadd45 β -infected mice. $n = 6$ per group. (F) Global DNA methylation ratio in Ad-GFP- or Ad-Gadd45 β -infected MPHs. $n = 4$ per group. (G and H) Methylation levels at the promoter regions of Dhx15 in Ad-GFP- or Ad-Gadd45 β -infected mouse livers (G) or MPHs (H). (I and J) Methylation levels at the promoter regions of PEPCK (I) and G6Pase (J) in Ad-GFP- or Ad-Gadd45 β -infected mouse livers. $n = 6$ per group. (K and L) Methylation levels at the promoter regions of PEPCK (K) and G6Pase (L) in Ad-GFP- or Ad-Gadd45 β -infected MPHs. $n = 4$ per group. (M) Promoter-specific methylation levels were analyzed by MeDIP-qPCR. The ratio of methylated DNA levels in livers from Dex- or vehicle control-treated mice is presented. $n = 8$ per group. (N) The percentage of DNA methylation in individual methylated cytosine sites in livers from Dex- or vehicle control-treated mice analyzed by pyrosequencing. $n = 8$ per group. (O) Promoter-specific methylation levels were analyzed by MeDIP-qPCR. The ratio of methylated DNA levels in livers from mice under fed or fasting conditions is presented. $n = 6$ per group. (P) The percentage of DNA methylation in individual methylated cytosine sites in livers from mice under fed or fasting conditions analyzed by pyrosequencing. $n = 6$ per group. (Q) ChIP-qPCR analysis showing the binding activity of phosphorylated CREB on the PGC-1 α promoter. MPHs were transfected with Ad-GFP or Ad-Gadd45 β for 24 h and then treated with forskolin (5 μ M) or vehicle control for another 2 h. $n = 4$ per group. (R) ChIP-qPCR analysis for binding of histones H3K9me3, H3K27me3, and H3K4me3 at the PGC-1 α promoter in MPHs infected with Ad-GFP or Ad-Gadd45 β . $n = 4$ per group. Data are represented as mean \pm SEM. *, $P < 0.05$; **, $P < 0.01$; ***, $P < 0.001$. Two-tailed Student's t test (C, E-M, O, and R); one-way ANOVA (B, D, N, P, and Q). Data are combined from four (B-D, F-H, K, L, Q, and R) independent experiments.

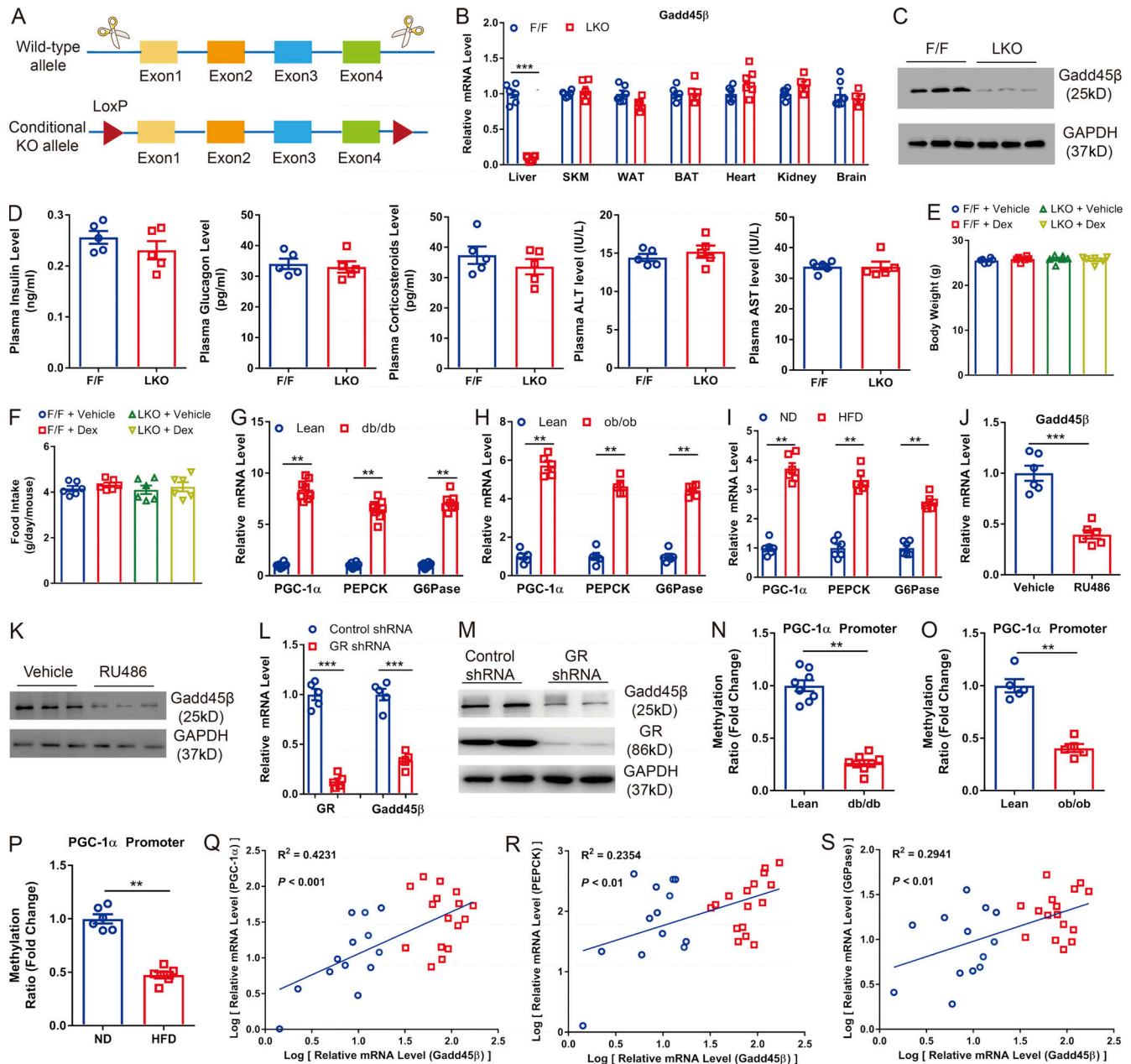


Figure S4. **Generation of Gadd45 β LKO mice and the methylation status and expression of hepatic gluconeogenic genes in diabetes.** (A) Gadd45 β F/F mice were generated by the CRISPR/Cas9 system with two loxP sites flanking exons 1–4 of the Gadd45 β gene. 8-wk-old male Gadd45 β F/F mice were administered AAV-GFP or AAV-Cre at a dose of 2.0×10^9 genome copies g^{-1} through tail vein injection. (B) Relative mRNA levels of Gadd45 β in various tissues from F/F and LKO mice. $n = 5$ per group. (C) Protein levels of Gadd45 β in the liver of F/F and LKO mice. (D) Plasma insulin, glucagon, corticosteroids, alanine aminotransferase, and aspartate aminotransferase levels between Gadd45 β F/F and LKO mice. $n = 5$ per group. (E and F) Body weights (E) and food intake (F) of Gadd45 β F/F or LKO mice treated with Dex (1.0 mg/kg) or vehicle control for 14 d. $n = 6$ per group. (G) Relative mRNA levels of PGC-1 α , PEPCK, and G6Pase in the livers of *db/db* and lean mice. $n = 8$ per group. (H) Relative mRNA levels of PGC-1 α , PEPCK, and G6Pase in the livers of *ob/ob* and lean mice. $n = 5$ per group. (I) Relative mRNA levels of PGC-1 α , PEPCK, and G6Pase in the livers of HFD-fed and normal diet (ND)-fed mice. $n = 6$ per group. (J and K) HFD-induced obese mice were treated with vehicle control or RU486 (25 mg/kg) for 7 d. mRNA and protein levels of Gadd45 β were analyzed by qPCR (J) and Western blotting (K), respectively. $n = 6$ per group. (L and M) HFD-induced obese mice were injected with control shRNA or GR shRNA through the tail vein for 10 d. mRNA and protein levels of Gadd45 β and GR were analyzed by qPCR (L) and Western blotting (M), respectively. $n = 5$ per group. (N–P) Promoter-specific methylation levels at the PGC-1 α promoter region were analyzed by MeDIP-qPCR in three types of diabetic mice. (Q–S) Pearson correlation analysis for the normalized Gadd45 β mRNA levels versus PGC-1 α mRNA levels (Q), PEPCK mRNA levels (R), and G6Pase mRNA levels (S) in human subjects ($n = 29$). Blue circle, normal; red square, T2DM. **, $P < 0.01$; ***, $P < 0.001$. Two-tailed Student's t test (B, D, G–J, L, and N–P); one-way ANOVA (E and F). Pearson correlation analysis (Q–S). Data are representative of two (B–P) independent experiments. BAT, brown adipose tissue; SKM, skeletal muscle. WAT, white adipose tissue.

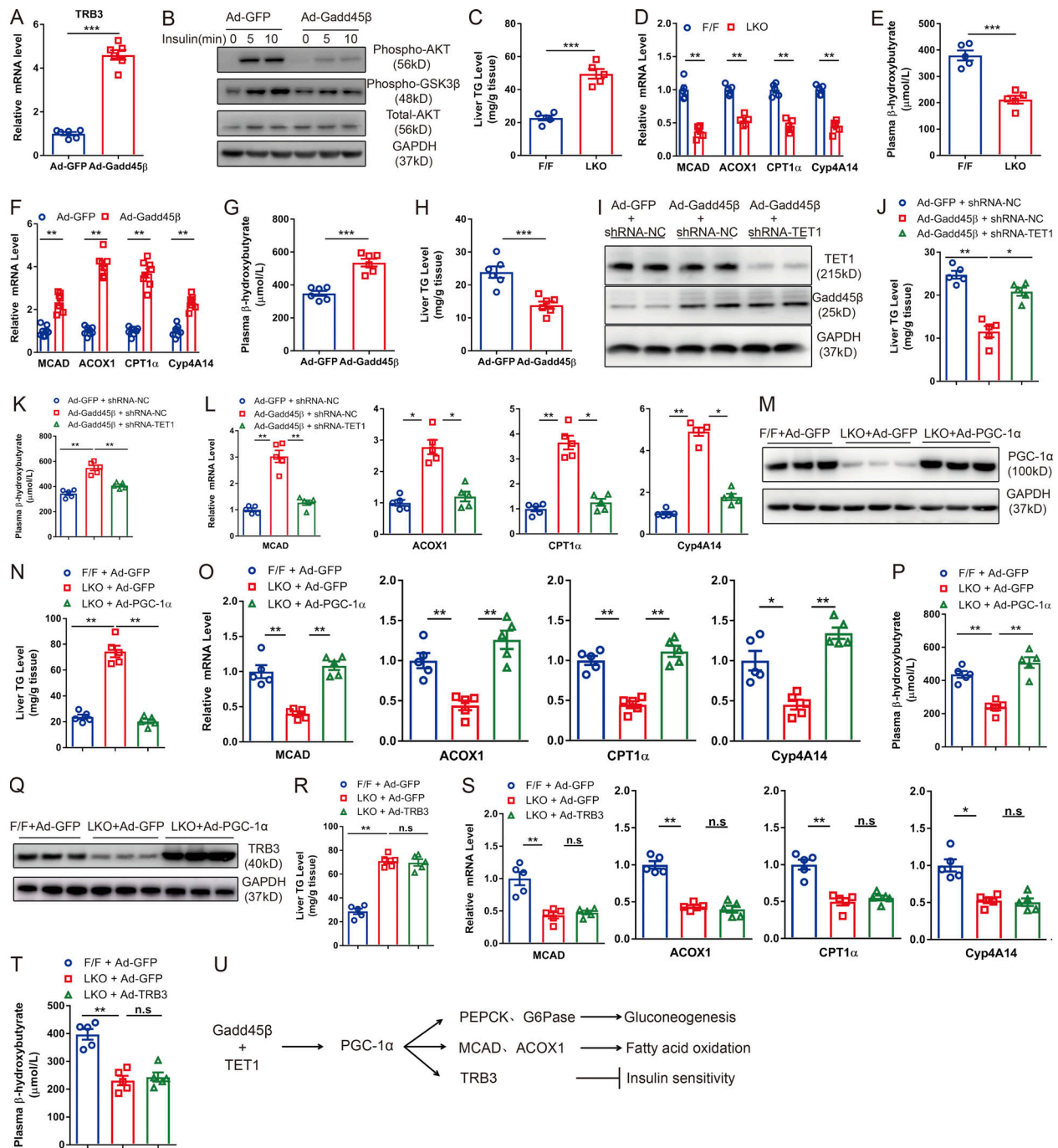


Figure S5. Hepatic insulin signaling and lipid metabolism in mice. (A) Relative mRNA levels of TRB3 in the livers of mice expressing Ad-GFP or Ad-Gadd45 β . $n = 6$ per group. (B) Western blots showing the insulin-stimulated phosphorylated AKT and GSK3 β in the livers of mice expressing Ad-GFP or Ad-Gadd45 β . (C) Hepatic TG content in 16-h fasting Gadd45 β F/F and LKO mice. $n = 5$ per group. (D) Relative mRNA levels of ACOX1, MCAD, CPT1 α , and Cyp4A14 in the livers of mice described in C. (E) Plasma β -hydroxybutyrate levels of the mice described in C. (F) Relative mRNA levels of ACOX1, MCAD, CPT1 α , and Cyp4A14 in the livers of C57BL/6 mice expressing Ad-GFP or Ad-Gadd45 β . $n = 6$ per group. (G and H) Plasma β -hydroxybutyrate levels (G) and hepatic TG contents (H) in mice expressing Ad-GFP or Ad-Gadd45 β . $n = 6$ per group. (I–L) C57BL/6 male mice were administered Ads as indicated for 10 d. Mice were fasted for 16 h before sacrifice. $n = 5$ per group. (I) Hepatic protein levels of TET1 or Gadd45 β in three groups of mice. (J) Hepatic TG contents. (K) Plasma β -hydroxybutyrate concentrations. (L) Relative mRNA expression of fatty acid oxidation–related genes. (M–P) Gadd45 β F/F or LKO mice were administered Ads containing GFP or PGC-1 α as indicated for 10 d. Mice were fasted for 16 h before sacrifice. $n = 5$ per group. (M) Hepatic protein levels of PGC-1 α in three groups of mice. (N) Hepatic TG contents. (O) Relative mRNA expression of fatty acid oxidation–related genes. (P) Plasma β -hydroxybutyrate concentrations. (Q–T) Gadd45 β F/F or LKO mice were administered Ads containing GFP or TRB3 as indicated for 10 d. Mice were fasted for 16 h before sacrifice. $n = 5$ per group. (Q) Hepatic protein levels of TRB3 in three groups of mice. (R) Hepatic TG contents. (S) Relative mRNA expression of fatty acid oxidation–related genes. (T) Plasma β -hydroxybutyrate concentrations. (U) Working model for the role of Gadd45 β /TET1 complex in the regulation of hepatic glucose and lipid metabolism in the fasted state. Data are represented as mean \pm SEM. *, $P < 0.05$; **, $P < 0.01$; ***, $P < 0.001$. Two-tailed Student’s t test (A and C–H); one-way ANOVA (J–L, N–P, and R–T). Data are representative of two (A–T) independent experiments.

Tables S1, S2, S3, and S4 are provided online. Table S1 shows the results of RNA-seq analysis of the genes up-regulated by Dex/vehicle control. Table S2 shows overlap of the up-regulated expressed genes from the livers of two mouse models (Dex/vehicle control and fasting/fed). Table S3 shows overlap of the down-regulated expressed genes from the livers of two mouse models (Dex/vehicle control and fasting/fed). Table S4 lists the clinical characteristics of human subjects.